

AFAPL-TR-71-52  
Volume I

AD 729439

# DESIGN OF MAXIMUM THRUST NOZZLES FOR GAS-PARTICLE FLOWS

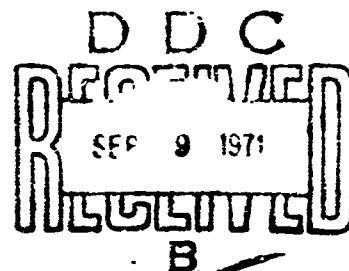
## VOLUME I. THEORETICAL DEVELOPMENT AND RESULTS

Arnold A. Elsbernd, Lt. Colonel, USAF, and Joe D. Hoffman

Jet Propulsion Center  
Purdue University  
Lafayette, Indiana 47907

TECHNICAL REPORT AFAPL-TR-71-52, VOLUME I

JUNE 1971



This document has been approved for public release and sale;  
its distribution is unlimited.

Reproduced by  
NATIONAL TECHNICAL  
INFORMATION SERVICE  
Springfield, Va. 22151

AIR FORCE AERO PROPULSION LABORATORY  
AIR FORCE SYSTEMS COMMAND  
WRIGHT-PATTERSON AIR FORCE BASE, OHIO

102

UNCLASSIFIED

Security Classification

## DOCUMENT CONTROL DATA - R &amp; D

(Security classification of title, body of abstract and indexing annotation must be entered when the overall report is classified)

1. ORIGINATING ACTIVITY (Corporate author) Purdue University Lafayette, Indiana 47907		2a. REPORT SECURITY CLASSIFICATION UNCLASSIFIED	
		2b. GROUP	
3. REPORT TITLE DESIGN OF MAXIMUM THRUST NOZZLES FOR GAS-PARTICLE FLOWS, VOLUME I, THEORETICAL DEVELOPMENT AND RESULTS			
4. DESCRIPTIVE NOTES (Type of report and, inclusive dates) Technical Report covering the period 15 July 1969 to 31 May 1971			
5. AUTHOR(S) (First name, middle initial, last name) Arnold A. Elsbernd, Lt. Colonel, USAF, and Joe D. Hoffman			
6. REPORT DATE June 1971		7a. TOTAL NO. OF PAGES 100	7b. NO. OF REFS 18
8a. CONTRACT OR GRANT NO. Air Force F33615-67-C-1068		8b. ORIGINATOR'S REPORT NUMBER(S)	
b. PROJECT NO. 3012			
c. Task 301209		9b. OTHER REPORT NO(S) (Any other numbers that may be assigned this report) AFAPL-TR-71-52, Volume I	
10. DISTRIBUTION STATEMENT This document has been approved for public release and sale; its distribution is unlimited.			
11. SUPPLEMENTARY NOTES		12. SPONSORING MILITARY ACTIVITY Air Force Aero Propulsion Laboratory Wright-Patterson Air Force Base, Ohio	
13. ABSTRACT An optimization analysis is presented for nozzles with gas-particle flows. The problem is formulated to maximize the axial thrust produced along the nozzle contour for a general isoperimetric constraint such as constant nozzle length or constant nozzle surface area. The effects of the ambient pressure are included in the thrust expression to be maximized. The characteristic and compatibility equations are developed and numerical techniques are presented for use in conjunction with the characteristic and compatibility equations. A solution procedure is presented which determines whether or not a given nozzle contour is an optimal solution and a relaxation technique is presented which adjusts the nozzle contour toward the optimal solution. Selected parametric studies are presented. These studies illustrate the effects of changing mesh size, particle size, particle mass flow rate, inlet angle, drag coefficients, heat transfer coefficients, throat radius of curvature, and the scale on the thrust performance and the nozzle geometry of the optimal, fixed length nozzle.			

DD FORM 1473 (PAGE 1)  
1 NOV 65  
S/N 0101-807-6811

UNCLASSIFIED

Security Classification

## NOTICES

When Government drawings, specifications, or other data are used for any purpose other than in connection with a definitely related Government procurement operation, the United States Government thereby incurs no responsibility nor any obligation whatsoever; and the fact that the Government may have formulated, furnished, or in any way supplied the said drawings, specifications, or other data, is not to be regarded by implication or otherwise as in any manner licensing the holder or any other person or corporation, or conveying any rights or permission to manufacture, use, or sell any patented invention that may in any way be related thereto.

SESSION NO.		
C/STI	WRITE SECTION <input checked="" type="checkbox"/>	
DOC	DIFF SECTION <input type="checkbox"/>	
DISSEMINATED	<input type="checkbox"/>	
AUTHORITY		
BY		
SUPERVISOR/ADMINISTRATIVE		
DATE: APR. 1971		
A		

Copies of this report should not be returned unless return is required by security considerations, contractual obligations, or notice on a specific document.

14. KEY WORDS	LINK A		LINK B		LINK C	
	ROLE	WT	ROLE	WT	ROLE	WT
Scremjet Technology						
Exhaust Nozzle						
Optimum Nozzle Design						
Method of Characteristics						
Calculus of Variations						
Numerical Relaxation Technique						
Computer Program						

DESIGN OF MAXIMUM THRUST  
NOZZLES FOR GAS-PARTICLE FLOWS  
VOLUME I. THEORETICAL DEVELOPMENT AND RESULTS

Arnold A. Elsbernd, Lt. Colonel, USAF, and Joe D. Hoffman

This document has been approved for public release  
and sale; its distribution is unlimited.

## ABSTRACT

An optimization analysis is presented for nozzles with gas-particle flows. The problem is formulated to maximize the axial thrust produced along the nozzle contour for a general isoperimetric constraint such as constant nozzle length or constant nozzle surface area. The effects of the ambient pressure are included in the thrust expression to be maximized. The characteristic and compatibility equations are developed and numerical techniques are presented for use in conjunction with the characteristic and compatibility equations. A solution procedure is presented which determines whether or not a given nozzle contour is an optimal solution and a relaxation technique is presented which adjusts the nozzle contour toward the optimal solution. Selected parametric studies are presented. These studies illustrate the effects of changing mesh size, particle size, particle mass flow rate, inlet angle, drag coefficients, heat transfer coefficients, throat radius of curvature, and the scale on the thrust performance and the nozzle geometry of the optimal, fixed length nozzle.

## FOREWORD

The present study is part of the program "An Analytical Study of the Exhaust Expansion System (Scramjet Scientific Technology)" being conducted by the Jet Propulsion Center, Purdue University, Lafayette, Indiana, under United States Air Force Contract No. F33615-67-C-1068, Project 3012, Task 301209, BPSN 7(63 301206 6205214). The Air Force program monitor was Capt. Gary J. Jungwirth of the Air Force Aero Propulsion Laboratory (AFAPL/RJT). This report presents the formulation, numerical solution procedure and the results of selected parametric studies of the design of maximum thrust nozzles with gas-particle flows. Volume II is the computer program user's manual.

This report was submitted by the authors on 31 May 1971.

Publication of this report does not constitute Air Force approval of the report's findings or conclusions. It is published only for the exchange and stimulation of ideas.

Gary J. Jungwirth  
Captain, USAF  
Project Engineer  
Ramjet Technology Branch  
Ramjet Engine Division  
AF Aero Propulsion Laboratory

## TABLE OF CONTENTS

	Page
SECTION I INTRODUCTION . . . . .	1
SECTION II ANALYSIS . . . . .	5
1. Introduction . . . . .	5
2. The Flow Model . . . . .	5
3. Formulation of the Optimization Problem . . . . .	9
4. Calculus of Variations . . . . .	12
a. Necessary Conditions . . . . .	12
b. The Euler Equations . . . . .	13
c. The Corner Condition . . . . .	16
d. The Transversality Condition . . . . .	17
5. Finite Difference Evaluation of $h_6$ and $h_7$ . . . . .	19
6. Summary of Resulting Equations . . . . .	21
SECTION III NUMERICAL METHODS . . . . .	25
1. Solution Procedure . . . . .	25
2. Flow Field Analysis . . . . .	25
3. Optimization Calculations . . . . .	27
4. Relaxation Technique . . . . .	28
SECTION IV PARAMETRIC STUDIES . . . . .	33
1. General . . . . .	33
2. Variation of Mesh Size . . . . .	33
3. Variation of Particle Size . . . . .	37
4. Variation of Particle Mass Flow Rate . . . . .	40
5. Variation of Inlet Angle . . . . .	42
6. Variation of the Drag and Heat Transfer Coefficients . . . . .	42
7. Variation of the Throat Radius of Curvature . . . . .	44
8. Nozzle Scaling . . . . .	48
SECTION V CONCLUSIONS . . . . .	51
APPENDIX I: DERIVATION OF THE EULER EQUATIONS . . . . .	53
APPENDIX II: CHARACTERISTIC AND COMPATIBILITY EQUATIONS . . . . .	61
APPENDIX III: THE CORNER CONDITION . . . . .	80
APPENDIX IV: THE TRANSVERSALITY CONDITION . . . . .	83
REFERENCES . . . . .	90

## LIST OF FIGURES

Figure	Page
1. General Optimization Model . . . . .	2
2. Gas-Particle Optimization Model . . . . .	10
3. Mesh Point Construction . . . . .	26
4. Nozzle Contour Behavior . . . . .	30
5. Error Function Behavior . . . . .	31
6. Effect of Particle Size on Final Contour . . . . .	38
7. Variation of Particle Mass to Gas Mass Ratio . . . . .	41
8. Inlet Angle Effects . . . . .	43
9. Effect of Drag Coefficient Variation . . . . .	45
10. Effect of Heat Transfer Coefficient Variation . . . . .	46
11. Effect of Throat Radius of Curvature . . . . .	47
12. Effect of Scaling . . . . .	49
13. Determinant for Finding Gas Characteristic Equations . .	68
14. Determinant for Finding Particle Characteristic Equations	77

## LIST OF TABLES

Table	Page
I. Result of Varying the Number of Initial-Line Points . . .	35
II. Computation Times . . . . .	36
III. Off Design Particle Size Analysis . . . . .	39
IV. Thrust Evaluation for Nozzle Scaling . . . . .	50

## SECTION I

### INTRODUCTION

Many propellant combinations produce condensed phases in the exhaust products. These condensed phases may be due to the introduction of metal additives designed to increase energy release. These condensed phases, however, introduce performance losses due to the non-equilibrium effects of heat transfer and drag between the gas and the condensed phase particles.

The first application of optimization techniques to the design of rocket nozzles was made by Guderley and Hantsch (1) for isentropic flow in 1955. Rao (2,3) simplified the analysis and applied the formulation of the problem to standard nozzles and to plug nozzles. Guderley (4) then extended the results to isentropic flows which allow entropy to vary between streamlines.

Figure 1 represents the general model used for formulating the optimization of standard axisymmetric nozzles. In the above analyses, the problem was formulated to provide maximum thrust across an exit control surface, BC, and employed a constant length design constraint. Since the formulation is limited to the exit control surface, no dissipative effects in the flow field are allowed and nozzle design constraints not directly related to the exit control surface are not available.

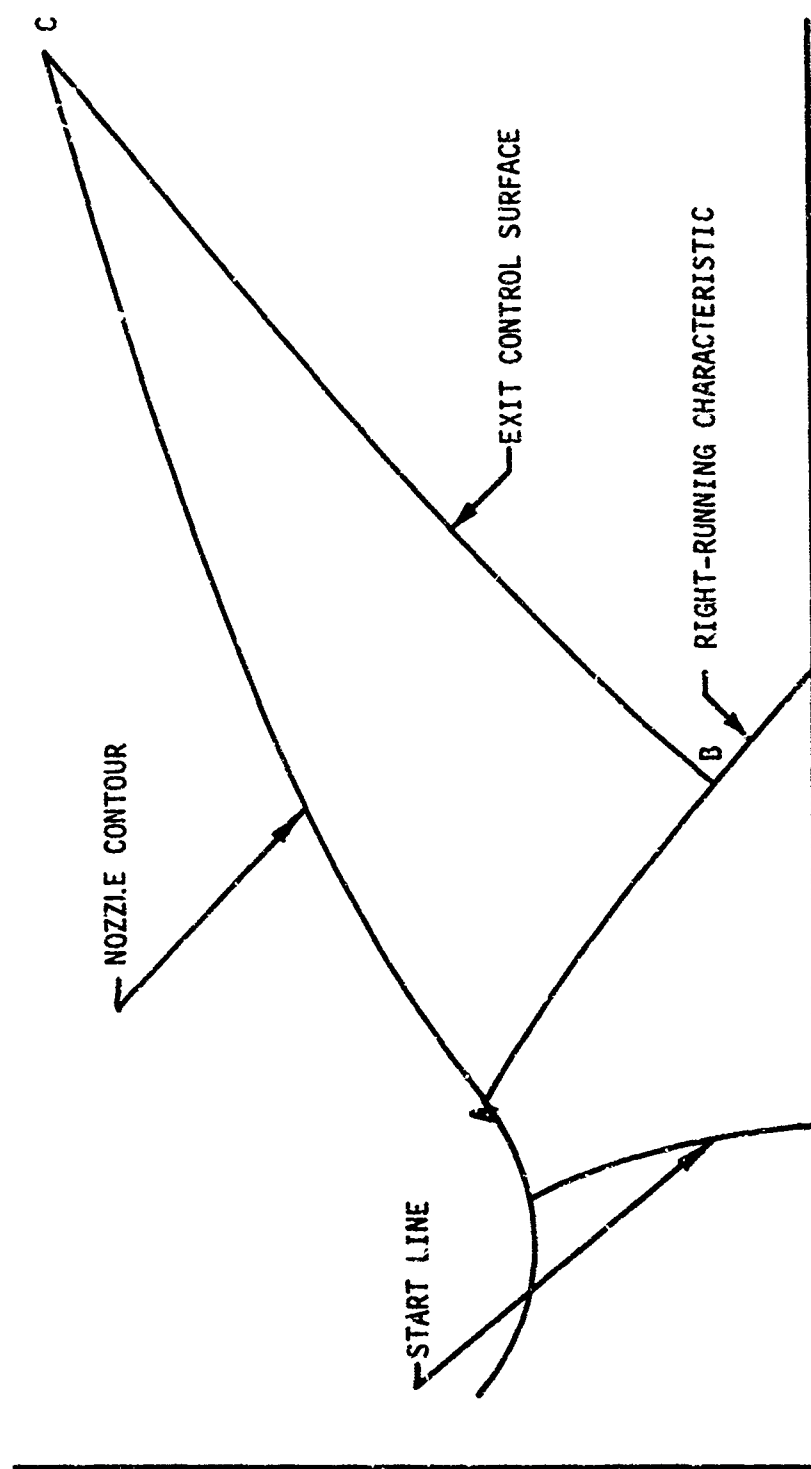


FIGURE 1. GENERAL OPTIMIZATION MODEL

Guderley and Armitage (5,6) formulated the optimization problem over the entire region ABC in order to use a constant surface area as a design constraint in lieu of constant length. This approach permits the use of a wide range of geometric design constraints. The complexity of the formulation and the numerical solution are greatly increased over the previous formulations.

The Guderley-Armitage approach can also be extended to dissipative flows since the entire region ABC is considered in the formulation. Hoffman and Thompson (7,8) formulated the problem for gas-particle flows and Hoffman (9,10) formulated the problem for reacting non-equilibrium flows. Further work was performed at Purdue University to develop the numerical schemes and to furnish working computer programs for the design of maximum thrust nozzles having flow fields with dissipative effects. Scofield and Hoffman (11) treated rotational or non-equilibrium simple dissociating gas flows, Humphreys, Thompson and Hoffman (12) treated plug nozzles with fixed inlet geometry, and Johnson, Thompson and Hoffman (13) treated plug nozzles with variable inlet geometry.

This work presents the formulation and numerical schemes developed to determine maximum thrust nozzle contours for nozzles with condensed particles in the flow field, and presents the results of an extensive parametric study. The optimization problem is formulated over the region ABC (Fig. 1), and follows that presented in Refs. (7,8). The method presented herein uses the calculus of variations to develop Lagrange multiplier equations, develops a numerical scheme to apply these equations to a previously calculated flow field in an assumed nozzle contour, determines an error function along the assumed wall, and calculates a new wall. This procedure is repeated until the error function goes to zero, and the

maximum thrust contour is obtained. An existing gas-particle flow field analysis program developed by Kliegel and Nickerson (14) was adapted to provide the evaluation of the flow properties in the nozzle.

## SECTION II

### ANALYSIS

#### 1. INTRODUCTION

In formulating thrust optimization problems, two basic approaches have been used. The first, and by far the easiest to use, maximizes the thrust written in terms of flow variables across an exit control surface. However, the application of this approach is limited since the formulation along the exit surface does not allow for dissipative flows or for constraints which cannot be related directly to the exit surface. In the second approach, the thrust is written in terms of forces acting along the wall contour AC in Figure 1 and the entire region ABC is considered in the problem. This approach permits the consideration of flows with dissipative effects such as gas-particle drag or finite rate chemistry. This second approach will be employed in this work.

#### 2. THE FLOW MODEL

The governing equations for the axisymmetric gas-particle flow analysis are given in Ref.(15). These equations are a gas continuity equation, two system momentum equations, a system energy equation, a particle continuity equation, two particle momentum equations and a particle energy equation.

$$(y\rho u)_x + (y\rho v)_y = 0 \quad (1)$$

$$\rho(uu_x + vu_y) + p_x + A\rho_p(u - u_p) = 0 \quad (2)$$

$$\rho(uv_x + vv_y) + p_y + A\rho_p(v - v_p) = 0 \quad (3)$$

$$up_x + vp_y - a^2(u\rho_x + v\rho_y) - AB\rho_p = 0 \quad (4)$$

$$(y\rho_p u_p)_x + (y\rho_p v_p)_y = 0 \quad (5)$$

$$\rho_p[u_p(u_p)_x + v_p(u_p)_y - A(u - u_p)] = 0 \quad (6)$$

$$\rho_p[u_p(v_p)_x + v_p(v_p)_y - A(v - v_p)] = 0 \quad (7)$$

$$\rho_p[u_p(h_p)_x + v_p(h_p)_y - \frac{2}{3}AC(T - T_p)] = 0 \quad (8)$$

The parameters A, B and C were defined for convenience and represent particle drag and energy parameters.

$$A = (9f_u)/(2m_p r_p^2) \quad (9)$$

$$B = (\gamma - 1)[(u - u_p)^2 + (v - v_p)^2 - \frac{2}{3}C(T - T_p)] \quad (10)$$

$$C = (gC_p)/(f Pr) \quad (11)$$

where

$$f = C_D/(C_D)_{\text{Stokes}} \quad (12)$$

$$g = Nu/(Nu)_{\text{Stokes}} \quad (13)$$

Assumptions are made that the parameters A and C are constant at least locally in the flow field, and relationships defining T, T<sub>p</sub> and a<sup>2</sup> are

$$T = p/\rho R \quad (14)$$

$$T_p = T_p^0 + \frac{1}{C_c} (h_p - h_p^0) \quad (15)$$

$$a^2 = \frac{\gamma p}{\rho} \quad (16)$$

$h_p^0$  and  $T_p^0$  represent the reference enthalpy and temperature respectively, and  $C_c$  is the specific heat of the condensed phase.  $C_c$  depends on the phase and is equal to  $C_p$  for liquid particles,  $\infty$  during phase changes, and  $C_v$  for solid particles.

Using equations (9) through (16), the eight governing equations, (1) through (8), can be expressed in terms of two independent and eight dependent variables. This suggests the use of the Method of Characteristics for the solution of the flow field problem. The following characteristic and compatibility equations are obtained when the Method of Characteristics is applied to the eight governing equations (1) through (8).

Along the gas streamline

$$\frac{dy}{dx} = \frac{v}{u} \quad (17)$$

$$\rho u du + \rho v dv + dp = -A \rho_p [(u - u_p)dx + (v - v_p)dy] \quad (18)$$

$$u dp - a^2 u dp = AB \rho_p dx \quad (19)$$

Along Mach lines

$$\frac{dy}{dx} = \tan(\theta \mp \alpha) \quad (20)$$

$$a^2(v du - u dv) \pm \frac{a^2}{\rho} \cot \alpha dp = (u dy - v dx) \frac{a^2 v}{y} - A \frac{\rho_p}{\rho} \left\{ B(u dy - v dx) + a^2 [(u - u_p)dy - (v - v_p)dx] \right\} \quad (21)$$

Along Particle Streamlines

$$\frac{dy}{dx} = \frac{v_p}{u_p} \quad (22)$$

$$u_p du_p = A(u - u_p) dx \quad (23)$$

$$u_p dv_p = A(v - v_p) dx \quad (24)$$

$$u_p dh_p = \frac{2}{3} AC(T - T_p) dx \quad (25)$$

where  $\theta$  is the flow angle and  $\alpha$  is the Mach angle. The upper signs in equations (20) and (21) refer to right-running Mach lines and the lower signs refer to left-running Mach lines.

This system of equations provides seven equations along four distinct characteristic directions, and thus cannot be used alone to solve for eight variables. The reason for the deficiency has been explained by Sauerwein and Fendell (16) as being the assumption that particles do not contribute to the pressure. This results in only one distinct characteristic direction for the particle equations, the direction of the particle streamline. However, it can be seen that the particle density term in the particle continuity equation is also dependent on the divergence of streamlines. The absence of a pressure term prevents expression of the divergence in a characteristic set of equations.

Further examination of the system of equations (17) through (25) reveals that if the particle density can be determined by other means, the number of dependent variables is reduced to seven, and the system of equations is adequate. For this purpose, a stream function is introduced. Since the total amount of particles passing between the centerline and a given particle streamline must remain constant and the distribution of particles passing the initial-value line can be determined, an integration technique can be applied to determine particle density at each

point in the flow field. With the particle density determined, the remaining seven variables can be determined by application of the characteristic and compatibility equations (17) through (25).

In the above technique, it is necessary to determine the particle streamline to find the particle density. However, the particle streamline depends on particle velocities, which have not yet been determined. Thus, it is necessary to iterate the solution at each point until a sufficient accuracy is achieved.

### 3. FORMULATION OF THE OPTIMIZATION PROBLEM

In the problem of obtaining a maximum thrust nozzle, only changes in the nozzle wall between points A and C (Fig. 2) in the supersonic region are considered. The contour of the nozzle inlet and throat region are assumed to be fixed. The boundary of the problem consists of three line segments. The nozzle wall defines the first, AC. Since the nozzle contour upstream of A is fixed, the flow field upstream of a right-running characteristic attached at A is independent of the optimization problem, and the boundary AB is defined along a right-running characteristic. The third line segment, BC, closes the region and intersects the line AC at the end of the nozzle. No other restrictions are made on this line in the formulation of the problem. However, the line BC is represented as a left-running characteristic in Figure 2 because the solution of the calculus of variations equations results in the characteristic equation for this line, as shown later in equation (64).

The particles flowing through the nozzle do not follow the wall contour, and there will be a region near the wall which contains only

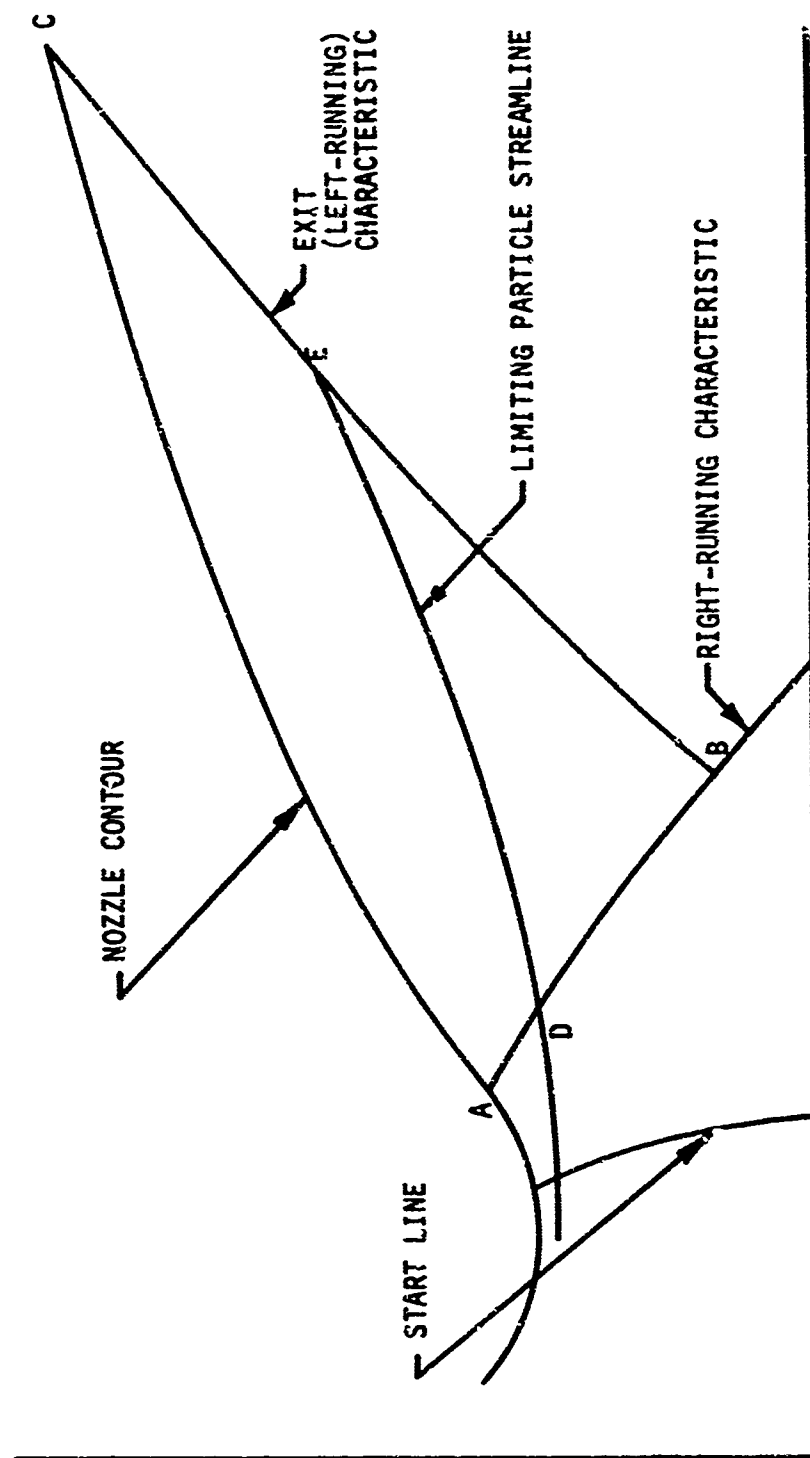


FIGURE 2. GAS-PARTICLE OPTIMIZATION MODEL

gas. The limiting particle streamline is represented in Figure 2 by the line DE. By definition the nozzle is not optimum if the limiting particle streamline impinges on the nozzle wall since the nozzle would be physically damaged, and in the case where the maximum thrust solution tends to result in impingement, it is necessary to change the inlet and throat region geometry sufficiently to provide the necessary separation.

The thrust developed along the nozzle wall is given by

$$\frac{F}{2\pi} = \int_A^C (p - p_0) \eta \eta' dx \quad (26)$$

where  $\eta$  is the radial coordinate of the wall and is a function of  $x$ . This quantity is to be maximized. However, there are several restrictions which must be imposed on the solution. The first requires that the wall be a gas streamline. Thus,

$$u \eta' - v = 0 \quad \text{on AC} \quad (27)$$

Equation (27) is multiplied by  $\eta \rho$  for convenience in subsequent analysis to give the equivalent expression

$$\eta \rho (u \eta' - v) = 0 \quad \text{on AC} \quad (28)$$

The second restriction is a constraint on the nozzle wall such as a constant length, a constant arc length, etc. For problems of general interest, this isoperimetric constraint can be expressed in terms of  $\eta$ ,  $\eta'$  and  $p$

$$\int_A^C G(\eta, \eta', p) dx - \text{Constant} = 0 \quad \text{on AC} \quad (29)$$

Finally, the governing equations (1) through (8) are restrictions throughout the region. Using  $L_i$  to represent the eight governing equations, the functional which is to be maximized is

$$I = \int_A^C [(p - p_0)nn' + C_1 G + C_2 np(un' - v)] dx + \iint_{ABC} \sum_{i=1}^8 h_i L_i dy dx \quad (30)$$

where  $C_1$  is a constant Lagrange multiplier,  $C_2$  is a Lagrange multiplier which is a function of  $x$ , and  $h_i$ , ( $i = 1, 8$ ), are Lagrange multipliers which are functions of  $x$  and  $y$ . The constant in the isoperimetric constraint does not affect the optimization problem, and therefore has been dropped from  $I$ . For convenience in the algebraic development, the following definitions are made:

$$H_1 = (p - p_0)nn' + C_1 G + C_2 np(un' - v) \quad (31)$$

$$H_2 = \sum_{i=1}^8 h_i L_i \quad (32)$$

#### 4. CALCULUS OF VARIATIONS

a. Necessary Conditions. Calculus of variations provides a set of conditions which must be satisfied if the optimum solution has been achieved. Necessary conditions include the Euler equations applicable to the region of interest, the transversality condition applicable along the boundaries, the corner condition applicable to corners formed by the intersection of two boundary line segments, and the Erdmann-Weierstrass condition applicable to corner lines in region ABC. In a supersonic nozzle, physical considerations rule out the class of solutions

which include corner lines; thus the Erdmann-Weierstrass condition is not used in this formulation and the first three conditions are considered sufficient.

b. The Euler Equations. The Euler equations, as given by Hiele (17), are

$$\frac{\partial H_2}{\partial z_k} - \frac{\partial}{\partial x} \left\{ \frac{\partial H_2}{\partial p_k} \right\} - \frac{\partial}{\partial y} \left\{ \frac{\partial H_2}{\partial q_k} \right\} = 0 \quad (k = 1, 2, \dots, 8) \quad (33)$$

where  $z_k$  represents the eight dependent variables  $p, \rho, u, v, h_p, \rho_p, u_p, v_p$ , and  $p_k$  and  $q_k$  represent the derivatives of these variables with respect to  $x$  and  $y$  respectively. The Euler equations are developed in Appendix I. The results are

$$\begin{aligned} -h_2 u_x - h_3 v_x - h_4 \frac{1}{\rho} (p_x - a^2 \rho_x) + y(h_1)_x + u(h_2)_x + v(h_2)_y = \\ = h_2 \frac{v}{y} + A \frac{\rho_p}{\rho} [h_2 - h_4 2(\gamma-1)(u-u_p) - h_6] \end{aligned} \quad (34)$$

$$\begin{aligned} -h_2 u_y - h_3 v_y - h_4 \frac{1}{\rho} (p_y - a^2 \rho_y) + y(h_1)_y + u(h_3)_x + v(h_3)_y = \\ = h_3 \frac{v}{y} + A \frac{\rho_p}{\rho} [h_3 - h_4 2(\gamma-1)(v-v_p) - h_7] \end{aligned} \quad (35)$$

$$\begin{aligned} h_4 u_x + h_4 v_y + h_4 \frac{a^2}{\rho} (u_p x + v_p y) + (h_2)_x + (h_3)_y + u(h_4)_x + \\ + v(h_4)_y = A \frac{\rho_p}{\rho} \frac{2}{3} \frac{C}{R} [(\gamma-1)h_4 - h_8] \end{aligned} \quad (36)$$

$$\begin{aligned} \frac{h_2}{\rho} p_x + \frac{h_3}{\rho} p_y + y u(h_1)_x + y v(h_1)_y + a^2 (h_2)_x + a^2 (h_3)_y = \\ = A \frac{\rho_p}{\rho} \left\{ \frac{2}{3} (\gamma-1) C \gamma [(\gamma-1)h_4 - h_8] + \gamma h_4 B - h_2(u-u_p) - h_3(v-v_p) \right\} \end{aligned} \quad (37)$$

$$\begin{aligned} h_6(u_p)_x + h_7(v_p)_x + h_8(h_p)_x - y(h_5)_x - u_p(h_6)_x - v_p(h_6)_y = \\ = A \left\{ h_2 - h_4 2(\gamma-1)(u-u_p) - h_6 \right\} - h_6 \frac{v_p}{y} \end{aligned} \quad (38)$$

$$\begin{aligned}
h_5(u_p)_y + h_7(v_p)_y + h_8(h_p)_y - y(h_5)_y - u_p(h_7)_x - v_p(h_7)_y = \\
= A\{h_3 - h_4 2(\gamma-1)(v-v_p) - h_7\} - h_7 \frac{v_p}{y} \quad (39)
\end{aligned}$$

$$u_p(h_8)_x + v_p(h_8)_y = \frac{2}{3} \frac{AC}{C_c} \{h_8 - (\gamma-1)h_4\} + h_8 \frac{v_p}{y} \quad (40)$$

$$\{u_p(h_5)_x + v_p(h_5)_y\} = A\{h_2(u - u_p) + h_3(v-v_p) - h_4B\} \quad (41)$$

In equations (38) through (41) the particle density function,  $\rho_p$ , has been factored out. It must be remembered that these equations apply only in the region where particles are present, region BDE. Since the dependent variables are determined independently of the optimization problem, they can be considered as known values during the evaluation of the Euler equations. Thus equations (34) through (41) constitute eight equations with eight unknown variables,  $h_1$  through  $h_8$ . Application of the Method of Characteristics (See Appendix II) results in a set of seven compatibility equations applicable along four distinct characteristic directions.

Along the gas streamline

$$\frac{dy}{dx} = \frac{v}{u} \quad (42)$$

$$\begin{aligned}
& - h_2 du - h_3 dv - h_4 \frac{1}{\rho} (dp - a^2 d\rho) + y dh_1 + u dh_2 + \\
& + v dh_3 = \left\{ h_2 \frac{v}{y} + A \frac{\rho_p}{\rho} [h_2 - h_4 2(\gamma-1)(u-u_p) - h_6] \right\} dx + \\
& + \left\{ h_3 \frac{v}{y} + A \frac{\rho_p}{\rho} [h_3 - h_4 2(\gamma-1)(v-v_p) - h_7] \right\} dy \quad (43)
\end{aligned}$$

$$\begin{aligned}
& (h_2 v - h_3 u) dv + h_2 \frac{1}{\rho} dp - (\gamma-1) u a^2 h_4 \frac{1}{\rho} d\rho + u dh_1 - \\
& - u a^2 dh_4 = \left\{ -a^2 h_4 \frac{v}{y} - a^2 A \frac{\rho}{\rho} \frac{2}{3} \frac{C}{R} [(\gamma-1) h_4 - h_8] + \right. \\
& + A \frac{\rho}{\rho} \frac{2}{3} (\gamma-1) CT [(\gamma-1) h_4 - h_8] + A \frac{\rho}{\rho} [\gamma h_4 B - h_2(u-u_p) - h_3(v-v_p)] \\
& \left. - A \frac{\rho}{\rho} (h_2 \frac{dy}{dx} - h_3)(v-v_p) \right\} dx \quad (44)
\end{aligned}$$

Along gas Mach lines

$$\frac{dy}{dx} = \tan(\theta \mp \alpha) \quad (45)$$

$$\begin{aligned}
& h_2 du + h_3 dv + h_4 \frac{1}{\rho} (dp - a^2 d\rho) - y dh_1 \mp \tan \alpha (v dh_2 - u dh_3) = \\
& = \pm \tan \alpha \left\{ h_3 \frac{v}{y} dx + A \frac{\rho}{\rho} [h_3 - h_4 2(\gamma-1)(v-v_p) - h_7] dx - \right. \\
& - h_2 \frac{v}{y} dy - A \frac{\rho}{\rho} [h_2 - h_4 2(\gamma-1)(u-u_p) - h_6] dy + \\
& \left. + \frac{1}{a^2} (udy - vdx) A \frac{\rho}{\rho} (\gamma-1) \left[ \frac{2}{3} CT \{ (\gamma-1) h_4 - h_8 \} + h_4 B \right] \right\} \quad (46)
\end{aligned}$$

where the upper signs in equations (45) and (46) are applicable along right-running characteristics and the lower signs are applicable along left-running characteristics.

Along particle streamlines

$$\frac{dy}{dx} = \frac{v_p}{u_p} \quad (47)$$

$$y u_p dh_5 = A [h_2(u-u_p) + h_3(v-v_p) - h_4 B] dx \quad (48)$$

$$\begin{aligned}
& u_p dh_6 + v_p dh_7 = h_6 du_p + h_7 dv_p + h_8 dh_p - y dh_5 - \\
& - A \left\{ h_2 - h_4 2(\gamma-1)(u-u_p) - h_6 \right\} dx + h_6 \frac{v_p}{y} dx - \\
& - A \left\{ h_3 - h_4 2(\gamma-1)(v-v_p) - h_7 \right\} dy + h_7 \frac{v_p}{y} dy \quad (49)
\end{aligned}$$

$$u_p dh_8 = \frac{2}{3} \frac{AC}{C} [h_8 - (\gamma-1)h_4]dx + h_8 \frac{v_p}{y} dx \quad (50)$$

Equations (42) through (50) are a system of seven compatibility equations which apply along four distinct characteristic directions. Since there are eight unknown dependent variables,  $h_1$  through  $h_8$ , a deficiency exists. Analysis of the equations shows that the system of equations does not permit evaluation of the variables  $h_6$  and  $h_7$  since derivatives of both appear in equation (49) only.

In this analysis,  $h_6$  and  $h_7$  will both be determined by finite difference evaluation in the vicinity of the point being considered.

c. The Corner Condition. The corner condition applicable at the corners A, B and C, as given by Miele (17), is

$$\Delta[H_1 - y' \frac{\partial H_1}{\partial y}] \delta x + \Delta[\frac{\partial H_1}{\partial y}] \delta y = 0 \quad (51)$$

where  $\Delta$  denotes the difference between the value of the quantity in brackets evaluated on each side of the corner and  $\delta x$  and  $\delta y$  signify small variations in  $x$  and  $y$ .

At point A, both  $x$  and  $y$  are fixed, and  $\delta x$  and  $\delta y$  are both zero; thus the corner condition is satisfied without new conditions. At point B, the quantity  $H_1$  is zero on both sides of the corner, and no new conditions result. At point C the variations  $\delta x$  and  $\delta y$  are arbitrary. Each must be able to vary independent of the other so the coefficients must be zero. Since  $H_1$  is zero along BC, the coefficients of  $\delta x$  and  $\delta y$  are zero on that side of the corner, and thus must also be zero at C when evaluated along AC.

$$H_1 - y' \frac{\partial H_1}{\partial y} = 0 \quad \text{at C} \quad (52)$$

$$\frac{\partial H_1}{\partial y'} = 0 \quad \text{at } C \quad (53)$$

Equations (52) and (53), when applied at point C (see Appendix III), result in

$$C_1 = - \frac{(p_c - p_0) \eta_c v_c}{u_c G_c} \quad (54)$$

$$C_{2_c} = - \frac{(p_c - p_0) \left[ 1 - \frac{v_c}{u_c G_c} \left( \frac{\partial G}{\partial \eta} \right)_c \right]}{\rho_c u_c} \quad (55)$$

d. The Transversality Condition. Along the boundaries, the transversality condition must be satisfied. The transversality equations are given in Appendix IV, and when applied along BC result in the set of equations:

$$h_3 - y' h_2 + h_4 (v - y' u) = 0 \quad (56)$$

$$h_1 y (v - y' u) - h_4 a^2 (v - y' u) = 0 \quad (57)$$

$$h_2 (v - y' u) - h_1 y y' = 0 \quad (58)$$

$$h_3 (v - y' u) + h_1 y = 0 \quad (59)$$

$$h_5 (y' u_p - v_p) = 0 \quad (60)$$

$$h_6 (y' u_p - v_p) + h_5 y' y = 0 \quad (61)$$

$$h_7 (y' u_p - v_p) - h_5 y = 0 \quad (62)$$

$$h_8 (y' u_p - v_p) = 0 \quad (63)$$

Substituting equations (57) through (59) into (56), we obtain, after simplification

$$y' = \frac{vu \pm a^2 \sqrt{M^2 - 1}}{u^2 - a^2} \quad \text{on BC} \quad (64)$$

Thus the transversality conditions specify that the line BC must be a left-running characteristic.

Since BC is a characteristic neither of the quantities  $v - y'u$  or  $y'u_p - v_p$  are zero. Equations (60) through (63) then reduce to

$$h_5 = 0 \quad (65)$$

$$h_6 = 0 \quad (66)$$

$$h_7 = 0 \quad (67)$$

$$h_8 = 0 \quad (68)$$

and equations (56) through (59), in addition to specifying the characteristic direction, become

$$h_1 y + h_2 (y'u - v) = 0 \quad (69)$$

$$h_1 y y' - h_3 (y'u - v) = 0 \quad (70)$$

$$h_1 y - a^2 h_4 = 0 \quad (71)$$

When the transversality condition is applied along the contour CA the following equations result:

$$h_1 = c_2 \quad (72)$$

$$uh_3 - v\dot{h}_2 + v\eta + u\dot{c}_1\dot{G}_p = 0 \quad (73)$$

$$\frac{dh_1}{dx} = \frac{du}{dx} + \frac{c_1}{\eta\rho u} \left[ G_\eta - \frac{d}{dx} \left( \frac{\partial G}{\partial \eta} \right) - \rho u \left( \frac{\partial G}{\partial p} \right) \left( \frac{dv}{dx} \right) \right] \quad (74)$$

## 5. FINITE DIFFERENCE EVALUATION OF $h_6$ AND $h_7$

The failure of the method of characteristics to produce eight compatibility equations necessitates the use of another method to solve for at least one unknown dependent variable. Since equation (49) includes both  $h_6$  and  $h_7$  in differential form, at least one of these must be obtained by another method in order to permit the solution of the other. In this analysis, both will be obtained in the vicinity of a point by using the appropriate Euler equations and the definition of a derivative.

The two Euler equations which contain partial derivatives of  $h_6$  and  $h_7$  are equations (38) and (39), repeated here for convenience

$$\begin{aligned} h_6(u_p)_x + h_7(v_p)_x + h_8(h_p)_x - y(h_5)_x - u_p(h_6)_x - v_p(h_6)_y = \\ = A \left\{ h_2 - h_4^2(\gamma-1)(u-u_p) - h_6 \right\} - h_6 \frac{v_p}{y} \end{aligned} \quad (38)$$

$$\begin{aligned} h_6(u_p)_y + h_7(v_p)_y + h_8(h_p)_y - y(h_5)_y - u_p(h_7)_x - v_p(h_7)_y = \\ = A \left\{ h_3 - h_4^2(\gamma-1)(v-v_p) - h_7 \right\} - h_7 \frac{v_p}{y} \end{aligned} \quad (39)$$

These equations can be written in a total differential form along the particle streamline if all the partial derivatives except the partial derivatives of  $h_6$  and  $h_7$  are known. To solve for the differential  $(u_p)_x$ , equation (6) and the total derivative of  $u_p$  are used,

$$u_p(u_p)_x + v_p(u_p)_y = A(u - u_p) \quad (6)$$

$$du_p = (u_p)_x dx + (u_p)_y dy \quad (75)$$

to obtain

$$(u_p)_x = \frac{A(u - u_p)dy - v_p du_p}{u_p dy - v_p dx} \quad (76)$$

Along the particle streamline,  $(u_p)_x$  is indeterminate. However, under the assumption of continuous derivatives,  $(u_p)_x$  can be evaluated along a gas right- or left-running characteristic and the results employed in equation (38).

In similar fashion

$$(v_p)_x = \frac{A(v - v_p)dy - v_p dv_p}{u_p dy - v_p dx} \quad (77)$$

$$(h_p)_x = \frac{\frac{2}{3} AC(T - T_p)dy - v_p dh_p}{u_p dy - v_p dx} \quad (78)$$

$$(u_p)_y = - \frac{A(u - u_p)dx - u_p du_p}{u_p dy - v_p dx} \quad (79)$$

$$(v_p)_y = - \frac{A(v - v_p)dx - u_p dv_p}{u_p dy - v_p dx} \quad (80)$$

$$(h_p)_y = - \frac{\frac{2}{3} AC(T - T_p)dx - u_p dh_p}{u_p dy - v_p dx} \quad (81)$$

Using equation (41) and the definition of the total derivative of  $h_5$ , the following expressions are derived:

$$(h_5)_x = \frac{A[h_2(u - u_p) + h_3(v - v_p) - h_4 B]dy - yv_p dh_5}{yu_p dy - yv_p dx} \quad (82)$$

$$(h_5)_y = - \frac{A[h_2(u-u_p) + h_3(v-v_p) - h_4 B]dx - y u_p dh_5}{y u_p dy = y v_p dx} \quad (83)$$

In equations (76) through (81), the evaluation of the partial derivatives involves only gas and particle properties. These values are known at all points in the flow field during evaluation of Lagrange multipliers, and are constant. However, evaluation of equations (82) and (83) requires the use of multiplier values not yet determined. Thus, values must first be assumed for the multipliers and the solution process iterated with updated values for the multipliers until a sufficiently accurate solution is obtained.

Treating the partial derivatives evaluated by equations (76) through (83) as constants, and restricting equations (38) and (39) to particle streamlines, we obtain the two compatibility-like equations:

$$u_p dh_6 = [-h_6(u_p)_x - h_7(v_p)_x - h_8(h_p)_x + y(h_5)_x + A \{h_2 - h_4 2(\gamma-1)(u-u_p) - h_6\} - h_6 \frac{v_p}{y}]dx \quad (84)$$

$$u_p dh_7 = [-h_5(u_p)_y - h_7(v_p)_y - h_8(h_p)_y + y(h_5)_y + A \{h_3 - h_4 2(\gamma-1)(v-v_p) - h_7\} - h_7 \frac{v_p}{y}]dx \quad (85)$$

## 6. SUMMARY OF RESULTING EQUATIONS

The set of equations which must be satisfied as necessary conditions for the calculus of variations includes eight Euler equations or their equivalent characteristic and compatibility system, three transversality equations along the nozzle contour AC, seven transversality equations

along the exit characteristic BC, and two corner condition equations at the point C. This is an overdetermined system of equations. One of the transversality equations along AC is not used in the computation of the Lagrange multipliers, and will thus be available for determination of an error function. This error function is used to modify the nozzle contour.

The resulting equations, in approximate order of usage for computation of multipliers, are repeated here. At the corner C

$$h_{1c} = c_{2c} = - \frac{(p_c - p_0) \left[ 1 - \frac{v_c}{u_c G_c} \left( \frac{\partial G}{\partial \eta} \right)_c \right]}{\rho_c u_c} \quad (86)$$

Along the exit characteristic BC

$$h_1 y + h_2 (y' u - v) = 0 \quad (69)$$

$$h_1 y y' - h_3 (y' u - v) = 0 \quad (70)$$

$$h_1 y - a^2 h_4 = 0 \quad (71)$$

$$h_5 = h_6 = h_7 = h_8 = 0 \quad (65-68)$$

Along the nozzle wall AC

$$\frac{dh_1}{dx} = \frac{du}{dx} - \frac{(p_c - p_0) \eta_c v_c}{u_c G_c} \frac{1}{\rho \eta} \left[ G_\eta - \frac{d}{dx} \left( \frac{\partial G}{\partial \eta} \right) - \rho u \left( \frac{\partial G}{\partial p} \right) \frac{dv}{dx} \right] \quad (74)$$

Along gas Mach lines

$$\frac{dy}{dx} = \tan(\theta \mp \alpha) \quad (45)$$

$$\begin{aligned}
& h_2 du + h_3 dv + h_4 \frac{1}{\rho} (dp - a^2 d\rho) - y dh_1 + \tan \alpha (v dh_2 - u dh_3) = \\
& = \pm \tan \alpha \left\{ h_3 \frac{v}{y} dx + A \frac{\rho_p}{\rho} [h_3 - h_4^2 (\gamma-1)(v-v_p) - h_7] dx - \right. \\
& \quad - h_2 \frac{v}{y} dy - A \frac{\rho_p}{\rho} [h_2 - h_4^2 (\gamma-1)(u-u_p) - h_6] dy + \\
& \quad + \frac{1}{a^2} (udy - vdx) A \frac{\rho_p}{\rho} (\gamma-1) \left[ \frac{2}{3} \text{CT} \left\{ (\gamma-1)h_4 - h_8 \right\} + h_4 B \right] \right\} \quad (46)
\end{aligned}$$

Along the gas streamline

$$\frac{dy}{dx} = \frac{v}{u} \quad (42)$$

$$\begin{aligned}
& - h_2 du - h_3 dv - h_4 \frac{1}{\rho} (dp - a^2 d\rho) + y dh_1 + u dh_2 + \\
& + v dh_3 = \left\{ h_2 \frac{v}{y} + A \frac{\rho_p}{\rho} [h_2 - h_4^2 (\gamma-1)(u-u_p) - h_6] \right\} dx + \\
& + \left\{ h_3 \frac{v}{y} + A \frac{\rho_p}{\rho} [h_3 - h_4^2 (\gamma-1)(v-v_p) - h_7] \right\} dy \quad (43)
\end{aligned}$$

$$\begin{aligned}
& (h_2 v - h_3 u) dv + h_2 \frac{1}{\rho} dp - (\gamma-1) u a^2 h_4 \frac{1}{\rho} d\rho + y u dh_1 - \\
& - u a^2 dh_4 = \left\{ - a^2 h_4 \frac{v}{y} - a^2 A \frac{\rho_p}{\rho} \frac{2}{3} \frac{C}{R} [(\gamma-1)h_4 - h_8] + \right. \\
& + A \frac{\rho_p}{\rho} \frac{2}{3} (\gamma-1) \text{CT} [(\gamma-1)h_4 - h_8] + A \frac{\rho_p}{\rho} [\gamma h_4 B - h_2(u-u_p) - \\
& \left. - h_3(v-v_p)] - A \frac{\rho_p}{\rho} (h_2 \frac{dy}{dx} - h_3)(v-v_p) \right\} dx \quad (44)
\end{aligned}$$

Along particle streamlines

$$\frac{dy}{dx} = \frac{v_p}{u_p} \quad (47)$$

$$y u_p dh_5 = A [h_2(u-u_p) + h_3(v-v_p) - h_4 B] dx \quad (48)$$

$$u_p dh_6 = [-h_6(u_p)_x - h_7(v_p)_x - h_8(h_p)_x + y(h_5)_x + \\ + A \{h_2 - h_4^2(\gamma-1)(u-u_p) - h_6\} - h_6 \frac{v}{y} p] dx \quad (84)$$

$$u_p dh_7 = [-h_6(u_p)_y - h_7(v_p)_y - h_8(h_p)_y + y(h_5)_y + \\ + A \{h_3 - h_4^2(\gamma-1)(v-v_p) - h_7\} - h_7 \frac{v}{y} p] dx \quad (85)$$

$$u_p dh_8 = \frac{2}{3} \frac{AC}{C_c} [h_8 - (\gamma-1)h_4] dx + h_8 \frac{v}{y} p dx \quad (50)$$

Finally, equation (73), which is not employed in the above set, is available as a check condition applicable along the nozzle wall to determine if the nozzle is optimum.

$$uh_3 - vh_2 + vn + uC_1G_p = 0 \quad (73)$$

## SECTION III

### NUMERICAL METHODS

#### 1. SOLUTION PROCEDURE

The solution procedure consists of estimating a nozzle contour, performing a flow field analysis, computing Lagrange multipliers, evaluating the check condition given by equation (73), and modifying the nozzle. This procedure is repeated using the modified nozzle contour as the estimated nozzle contour until the error criterion is satisfied. This section describes the program developed for use in the parametric studies.

The initial nozzle contour may be input in tabular form or calculated internally in the form of conical, parabolic or circular arc nozzles. The initial-value line, required to begin the supersonic flow field calculation, may be input as data or, for standard converging-diverging nozzles, can be generated internally based on the combustion chamber conditions.

#### 2. FLOW FIELD ANALYSIS

The flow field analysis utilizes the method of characteristics. Mesh points are located at intersections of left-running characteristics (LRCs) and right-running characteristics (RRCs). The reference streamline points are obtained by linear interpolation between reference points along the LRC and the RRC. See Figure 3. The mesh construction proceeds along LRCs beginning at either an initial-value point or an axis point, inserting points along RRCs from points on the previous LRC until the LRC intersects with the nozzle contour. Additional LRCs are constructed in this manner until the end of the nozzle contour is reached.

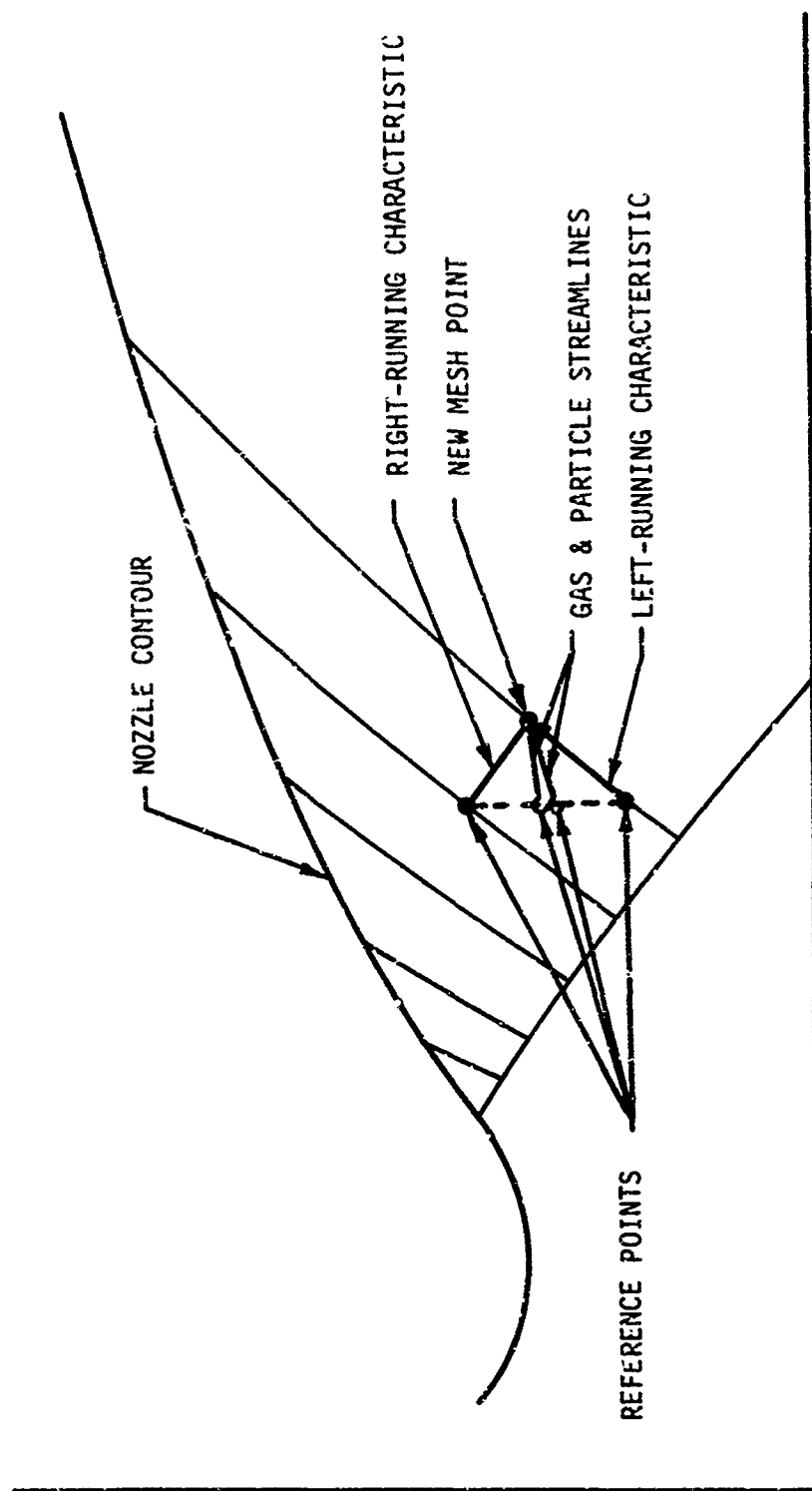


FIGURE 3. MESH POINT CONSTRUCTION

Axis points are located at the intersection of an RRC from the second point on the previous LRC and the axis. A limiting particle streamline point is calculated along each LRC and at least one additional point must lie between the limiting particle streamline and the nozzle contour. Point insertion routines are used to insert additional mesh points whenever the mesh size exceeds the values specified by input parameters. Whenever a mesh point is inserted along an RRC, a new LRC is begun at that point and proceeds to the nozzle contour before continuing on with the interrupted LRC. The point insertion routine is also used to locate the last point at the end of the nozzle contour.

During the flow field analysis, a secondary start line is constructed which follows an RRC from a point on the nozzle contour near point A (Fig. 2) to the axis. This secondary start line is used in subsequent iterations to reduce the calculation time by eliminating the recalculation of mesh points unaffected by the wall modification.

### 3. OPTIMIZATION CALCULATIONS

The optimization portion of the program begins with the determination of properties along an LRC which passes through the end point of the nozzle contour. This is accomplished by linear interpolation along the RRCs which connect points on either side of the exit characteristic. The Lagrange multipliers are then calculated along the exit characteristic and the method of characteristics is employed to determine the Lagrange multipliers throughout the flow field after reassembling the mesh construction in reverse order. A check condition, determined from equation (73) and expressed in terms of slopes, is calculated at wall points and an error function is determined.

#### 4. RELAXATION TECHNIQUE

The check condition, used to determine if the nozzle contour is optimum, will not in general be satisfied. After rewriting equation (73), an error parameter is defined:

$$E = \tan^{-1}(\eta') - \tan^{-1} \left( \frac{h_3 + C_1 G_p}{h_2 - \eta} \right) \quad (87)$$

By assuming that the remaining variables do not change appreciably with changes in wall slope,  $\eta'$ , the error parameter may be relaxed by calculating a new slope so that  $E$  will be zero. Thus, the new slope is given by

$$\eta' = \frac{h_3 + C_1 G_p}{h_2 - \eta} \quad (88)$$

This relaxation technique, first proposed by Major A. A. Taylor, USAF, while he was a graduate student at Purdue University, permits a simple integration to determine the relaxed nozzle contour.

$$\eta(x) = \eta(x_A) + \int_{x_A}^x \eta'(x) dx \quad (89)$$

Since the other variables do change when  $\eta'$  is changed, the solution is not exact, and the flow and optimization calculations must be iterated.

It was found that the relaxation scheme resulted in an overcorrection in the majority of cases. For this reason, a weighing factor was introduced to reduce the number of iterations, and thus the computation time. Thus, the modified contour slope  $\eta'$  is given by

$$\eta' = \eta_1' + 0.8(\eta_2' - \eta_1') \quad (90)$$

where  $\eta_2'$  represents the slope found by equation (88) and  $\eta_1'$  represents the slope of the original estimated nozzle contour. In addition, restrictions were placed on the calculation of the new nozzle contour to

prevent a change in slope greater than 10 degrees in either direction and to prevent negative slopes from being used.

The nozzle contour could become discontinuous if point A were fixed. This is avoided by permitting the point A to move along the throat radius of curvature until the slope at point A equals the slope calculated by equation (88). In the event point A moves upstream of the first point of the secondary start line, the flow field analysis will begin at the initial-value line for the next iteration and a new secondary start line beginning upstream of the new point A will be calculated.

Convergence of the nozzle contour is determined by the value of the error parameter,  $E$ , determined by equation (87). When  $E$  is less than the value of the input parameter  $TOL$  at each point along the nozzle contour, the convergence criterion is met and the program is terminated. If this convergence criterion is not met, the estimated nozzle contour is replaced by the modified nozzle contour and the solution is iterated beginning at the flow field analysis.

Figures 4 and 5 illustrate the behavior of this relaxation scheme. The sample case consists of a design to produce a maximum thrust nozzle 9.6 inches long with a throat radius of 1.2 inches and a throat radius of curvature of 2.4 inches. The initial estimate of the contour is a  $25^\circ$  conical nozzle. Aluminum oxide particles 4 microns in diameter with a mass flow rate 0.4 times the gas flow rate are specified. The gas properties are:  $\gamma = 1.28$ , molecular weight = 17.76, chamber pressure = 500 psia, chamber temperature = 6500°R, and ambient pressure = 3 psia. The convergence tolerance,  $TOL$ , was 0.05 degrees.

Seven iterations are required for convergence. The initial, second, fourth, and final nozzle contour are shown in Figure 4. The fourth and

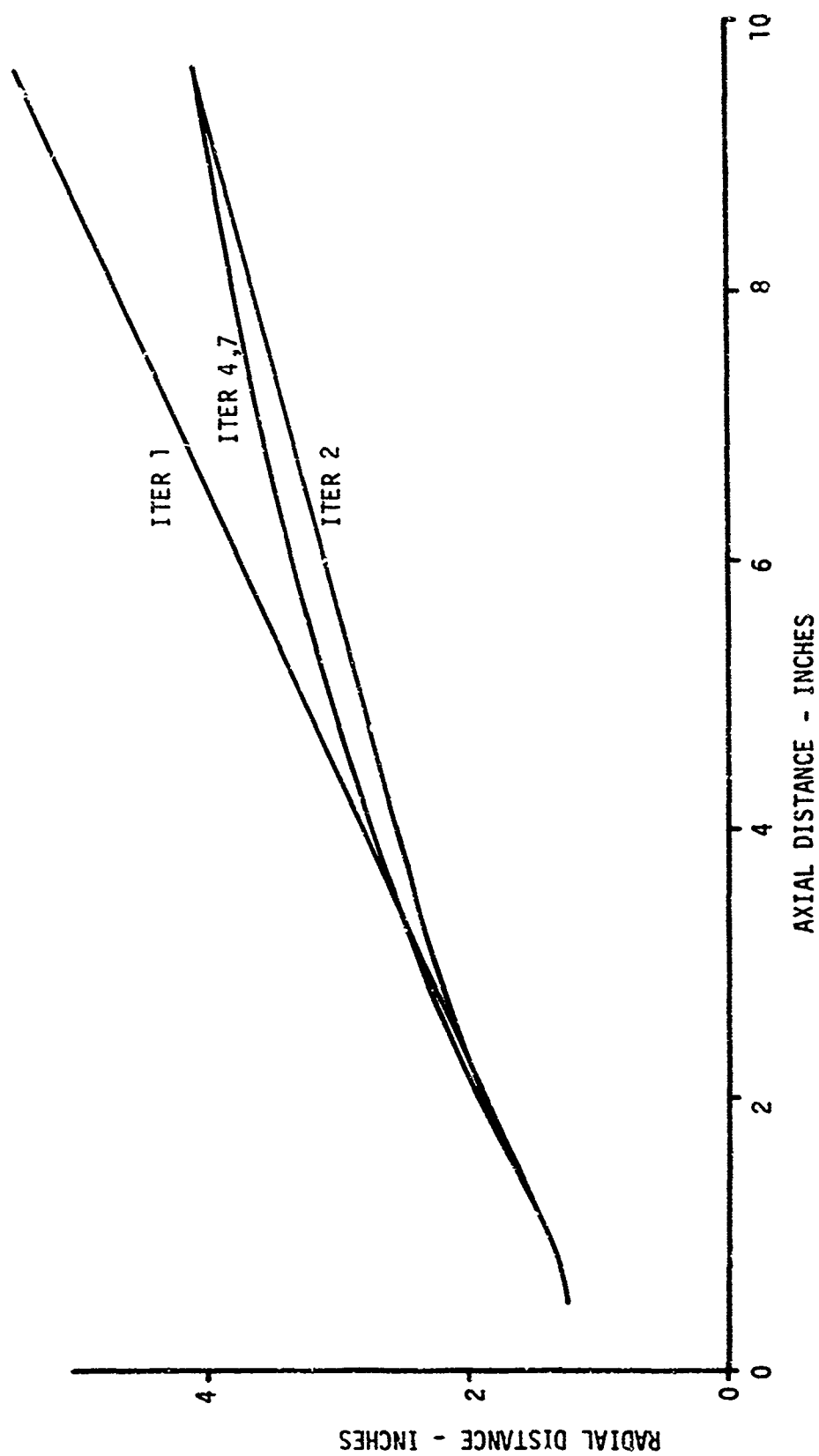


FIGURE 4. NOZZLE CONTOUR BEHAVIOR

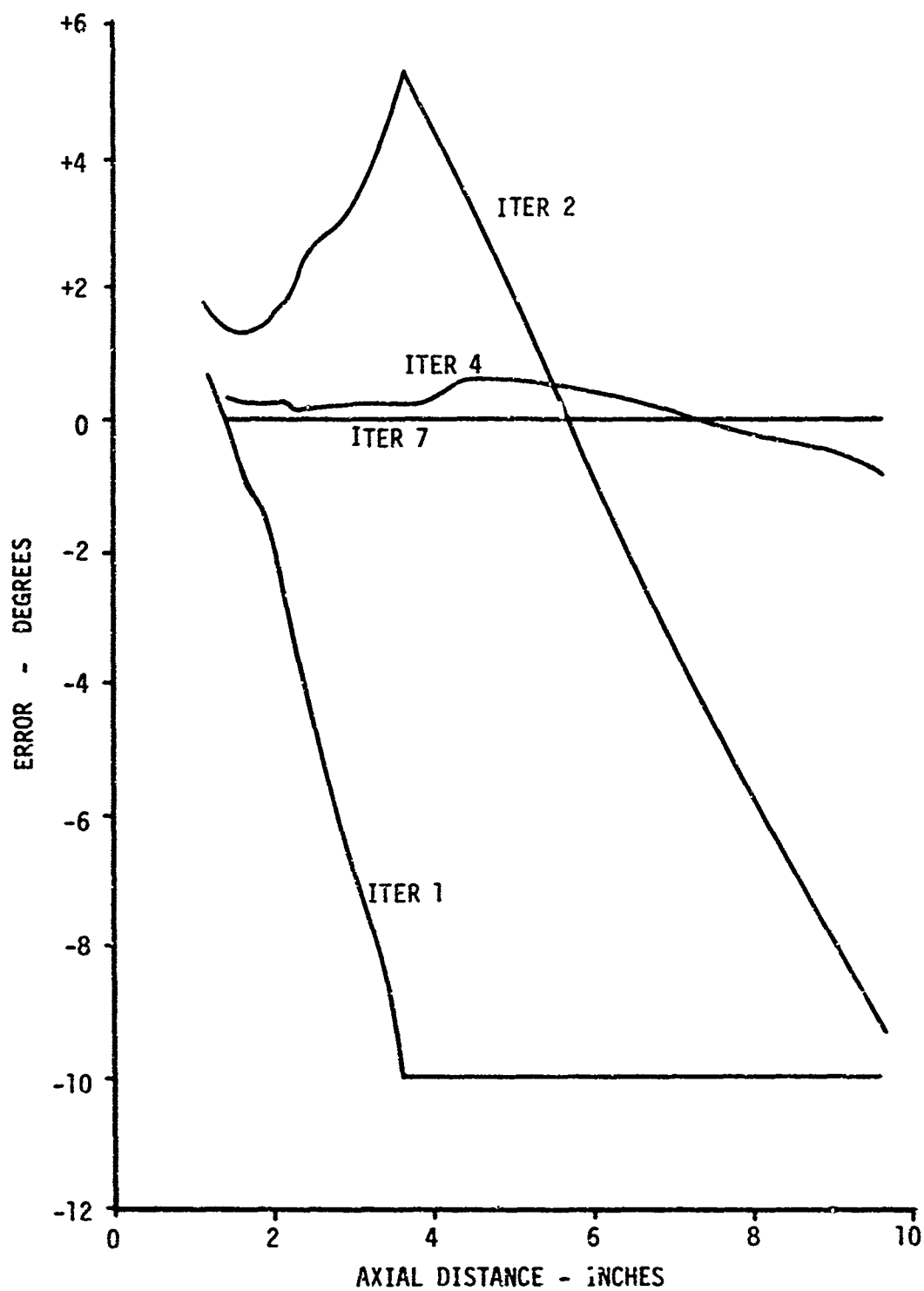


FIGURE 5. ERROR FUNCTION BEHAVIOR

final contours are almost identical. The corresponding error values are shown in Figure 5. The initial contour estimate of a conical nozzle resulted in large error values in the first iteration. However, the changes in nozzle contour were limited to ten degrees. The error values in the second iteration begin to show the overcorrection, then reverse where the first iteration correction was limited to ten degrees. The error values in the fourth iteration show a marked decrease, and by the seventh iteration are less than 0.05 degrees at all points.

## SECTION IV

### PARAMETRIC STUDIES

#### 1. GENERAL

A computer program, written in FORTRAN IV for the CDC 6500, was developed based on the analysis presented in Section II and the numerical methods presented in Section III. This computer program was designed to permit either the analysis of a given nozzle or the design of a maximum thrust nozzle subject to some geometric design constraint. The program user may choose to begin at an initial-value line in the supersonic region or with combustion chamber conditions. Output options permit selection of the amount of printed output and a punch capability designed to permit input of the computed nozzle contours and/or start lines into subsequent computations. A program description, description of input variables, and listing of several sample cases are given in Reference (18).

This section presents the results of parametric studies to determine the effect of varying several of the input parameters. For each parametric study, one variable was varied holding all others constant.

#### 2. VARIATION OF MESH SIZE

The method of characteristics mesh construction is controlled in two ways. First, the number of initial-line points (NILP) determines the size of the mesh near the initial value line and affects the mesh size throughout the flow field. Second, provisions are incorporated into the design program to limit the mesh size. In supersonic divergent nozzle flow, the mesh size tends to increase as the mesh construction proceeds

downstream. In the design program additional mesh points are inserted by the program whenever the dimension along a right-running characteristic exceeds the input value DR, the dimension along a left-running characteristic exceeds the input value DL, or the flow angle change along the nozzle contour exceeds the input variable DTWI.

For the first part of this parametric study, the values of DL, DR, and DTWI were set to relatively large values, thus inhibiting the mesh point insertion routines. A nozzle with a 1.2 inch throat radius, length of 9.6 inches and a 25 degree cone was selected. The ratio of the mass flow rate of the particles to the mass rate of flow of the gas was 0.4 and the size of the particles was 4 microns. Three values of NILP were used to vary the mesh size. The results are shown in Table I. The times required for each design were 342.9 sec, 593.8 sec, and 826.1 sec for NILP = 12, NILP = 16, and NILP = 20 respectively. These times could be reduced significantly if better initial contours were used. In all three cases, the initial contour is the same. The final nozzle contour was reached in one less iteration for NILP = 20.

Increasing NILP, and thus decreasing mesh size, results in almost identical final nozzle contours, with the nozzle exit radius slightly larger for increased NILP. The values for computed thrusts indicate a dependence on the mesh size. This can readily be seen by comparing the thrust computed for the first contour estimate in each case. Since these contours are identical, the difference can be attributed to the effect of the mesh size on the numeric scheme. Another effect can be noted in reviewing the thrust values. The final calculated thrust is typically slightly less than one or more of the intermediate calculated thrusts. However, this effect is slight, amounting to approximately 0.03% of the

TABLE I  
RESULTS OF VARYING THE NUMBER OF INITIAL LINE POINTS

CONTOUR ESTIMATE	EXIT RADIUS				THRUST	
	NILP = 12	NILP = 16	NILP = 20	NILP = 12	NILP = 16	NILP = 20
1st	5.431	5.431	5.431	3432.3	3434.6	3538.3
2nd	4.035	4.042	4.038	3545.6	3547.6	3550.0
3rd	3.935	3.940	3.945	3554.5	3556.3	3559.3
4th	3.998	4.017	4.030	3553.4	3557.0	3559.6
5th	4.027	4.047	4.061	3554.8	3556.0	3559.1
6th	4.035	4.051	4.064	3554.1	3555.6	3558.7
7th	4.037	4.056	4.065	3553.7	3555.5	3558.7
8th	4.037	4.056	4.064	3553.4	3555.4	
9th	4.037	4.057				

total thrust, and is within the accuracy of the numeric scheme. This suggests that the tolerance may be increased so that fewer iterations are required, since intermediate contours yield essentially the same thrust as the final.

A second part of this parametric study consisted of reducing the calculation times. For this purpose, four, five and six iterations (input parameter NITER) were performed with NILP = 12. Then the resulting computed nozzle contour was input into a design program with NILP = 20, and run until the error tolerance equal to  $0.05^\circ$  was satisfied. The results, shown in Table II, indicate a savings in total computational time can be achieved by first obtaining a better first estimate of the nozzle contour using a large mesh size. However, increasing the number of iterations with NILP = 12 to 5 and 6 does not reduce the number of iterations required with NILP = 20. A similar savings can be achieved by selecting an appropriate parabolic nozzle contour for the first estimate.

TABLE II  
COMPUTATION TIMES

NILP	NUMBER OF ITERATIONS WITH NILP = 12			
	0	4	5	6
12		178.6	217.3	253.6
20	826.1	360.6	361.6	359.7
	826.1	539.2	578.9	613.3

### 3. VARIATION OF PARTICLE SIZE

For the particle size studies, an eight inch circular arc nozzle with a  $30^\circ$  attachment angle and a four inch exit radius was used. The inlet to the throat was  $30^\circ$ . Particle sizes of 2, 4, 6, 8 and 10 microns were used. In all cases, the ratio of the mass rate of flow of the particles to the mass rate of flow of the gas was 0.4. The number of initial line points used was 20.

The final contours are shown in Figure 6. The optimized contours for the 4, 6, 8 and 10 micron particles are nearly the same, and the 2 micron optimized contour is not consistent with the others. Analysis of the numeric results revealed that the limiting particle streamline for the 2 micron case was near the nozzle contour, causing many linear interpolations in the process of computing limiting particle streamline points and wall points. This caused a loss of accuracy.

An analysis of off design conditions was made to determine the effect of particle size mismatch. The contours used in the analysis are the final contours just mentioned. In addition to the 2, 4, 6, 8 and 10 micron sizes, an analysis was also made using equal parts by mass of 2, 4, 6 and 8 micron particles such that the total ratio of mass flow rates was the same as for the analysis with one particle size. The results of these analyses are given in Table III. Also given are the nozzle radii at the exit for the optimum contours.

The use of the 2 micron wall resulted in lower thrust than for the other walls regardless of the size of particle used. This confirms the conclusion that the 2 micron design did not provide an optimum contour. The 4, 6, 8 and 10 micron walls provide the same thrust for each particle size used, within the accuracy of the numeric scheme of the program. The

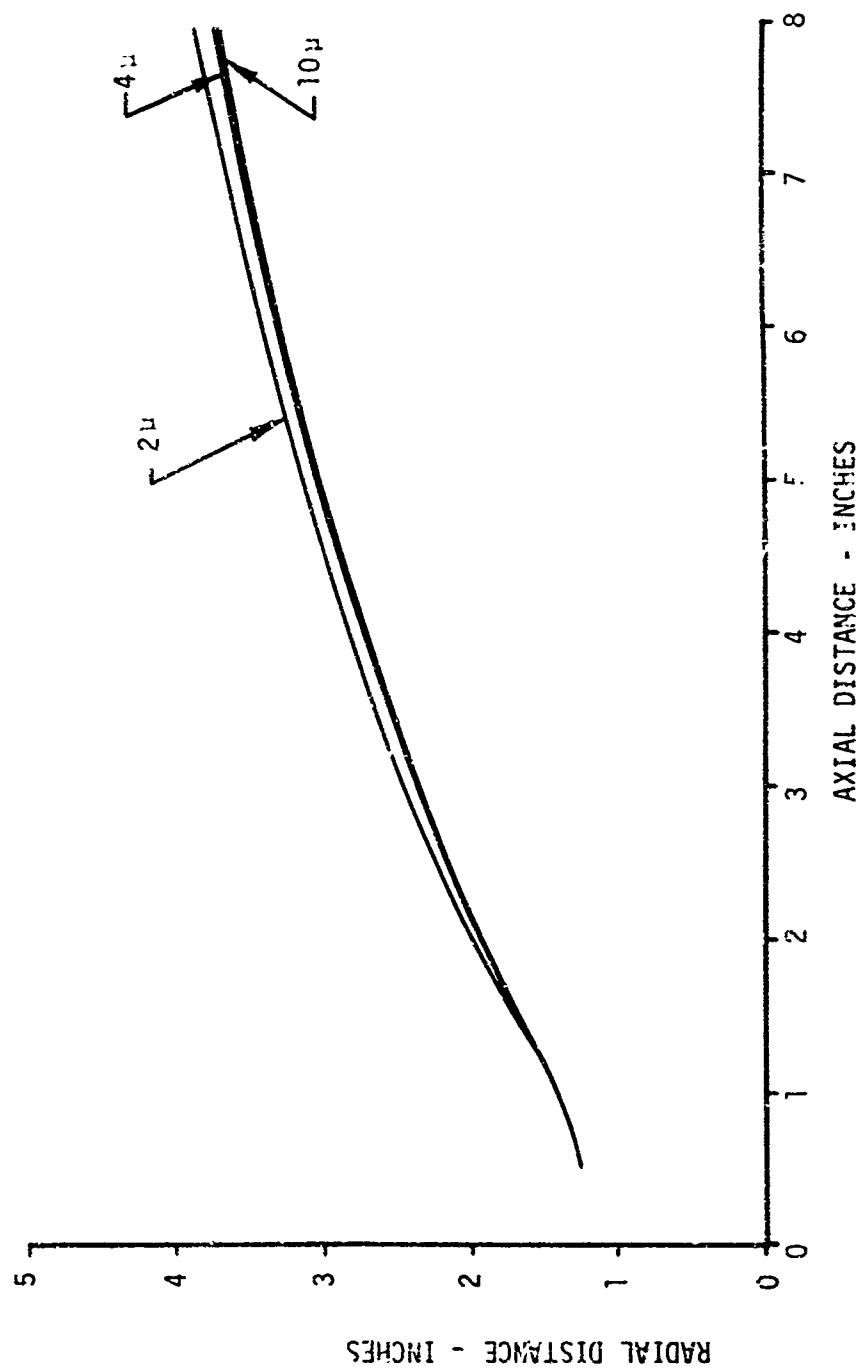


FIGURE 6. EFFECT OF PARTICLE SIZE ON FINAL CONTOUR

TABLE III  
OFF DESIGN PARTICLE SIZE ANALYSIS

PARTICLE SIZE USED IN ANALYSIS	EXIT RADIUS OF OPTIMUM NOZZLE	THRUST			
		PARTICLE SIZE USED IN DESIGN			
		2 $\mu$	4 $\mu$	6 $\mu$	10 $\mu$
2 $\mu$	3.861	3529.9	3542.0	3542.4	3542.7 3543.3
4 $\mu$	3.719	3498.6	3516.2	3516.3	3515.6 3515.9
6 $\mu$	3.706	3492.2	3507.4	3509.3	3508.3 3508.5
8 $\mu$	3.688	3486.3	3503.1	3504.8	3504.3 3504.4
10 $\mu$	3.661	3483.3	3497.0	3501.4	3498.6 3499.2
2-4-6-8		3511.8	3549.0	3543.4	3548.7 3549.1

parametric study required an inlet angle in the neighborhood of  $30^\circ$  as a compromise between the 2 micron and 10 micron requirements. Smaller inlet angles resulted in impingement of the 2 micron particles on the wall while larger angles provided large vertical momentum to the 10 micron particles, causing the particles to cross the centerline. The numeric integration of the particle mass could not be performed under these circumstances. Thus, in normal design programs for small particle sizes, an inlet angle of  $45^\circ$  is recommended to provide a greater separation between the nozzle contour and the limiting particle streamline.

The use of larger particle sizes results in less thrust, reflecting greater dissipative effects. The higher thrust computed for the mixture of four particle sizes is due in part to the use of some smaller particle sizes, and in part the increase in mesh points caused by insertion of a mesh point at each limiting particle streamline. The same effect was noted in the mesh size parametric studies.

#### 4. VARIATION OF PARTICLE MASS FLOW RATE

In this parametric study, the ratio of the mass rate of flow of the particles to the mass rate of flow of the gas (WPWGT) was set at 0.1, 0.4, 0.7, and 1.0. For the larger value of WPWGT, the effects of the particles near the throat region result in moving the sonic line downstream. For this reason, the initial-value line was shifted downstream by adjusting the input variables THIW and ZAX. The nozzle is an 8 inch nozzle with the initial contour assumed to be a circular arc attached at a  $30^\circ$  angle and with an exit radius of 4 inches. The particle size used was 4 microns. NLTP was 12

The results, shown in Figure 7, indicate that greater amounts of particles require more expansion to maximize the thrust. This phenomenon

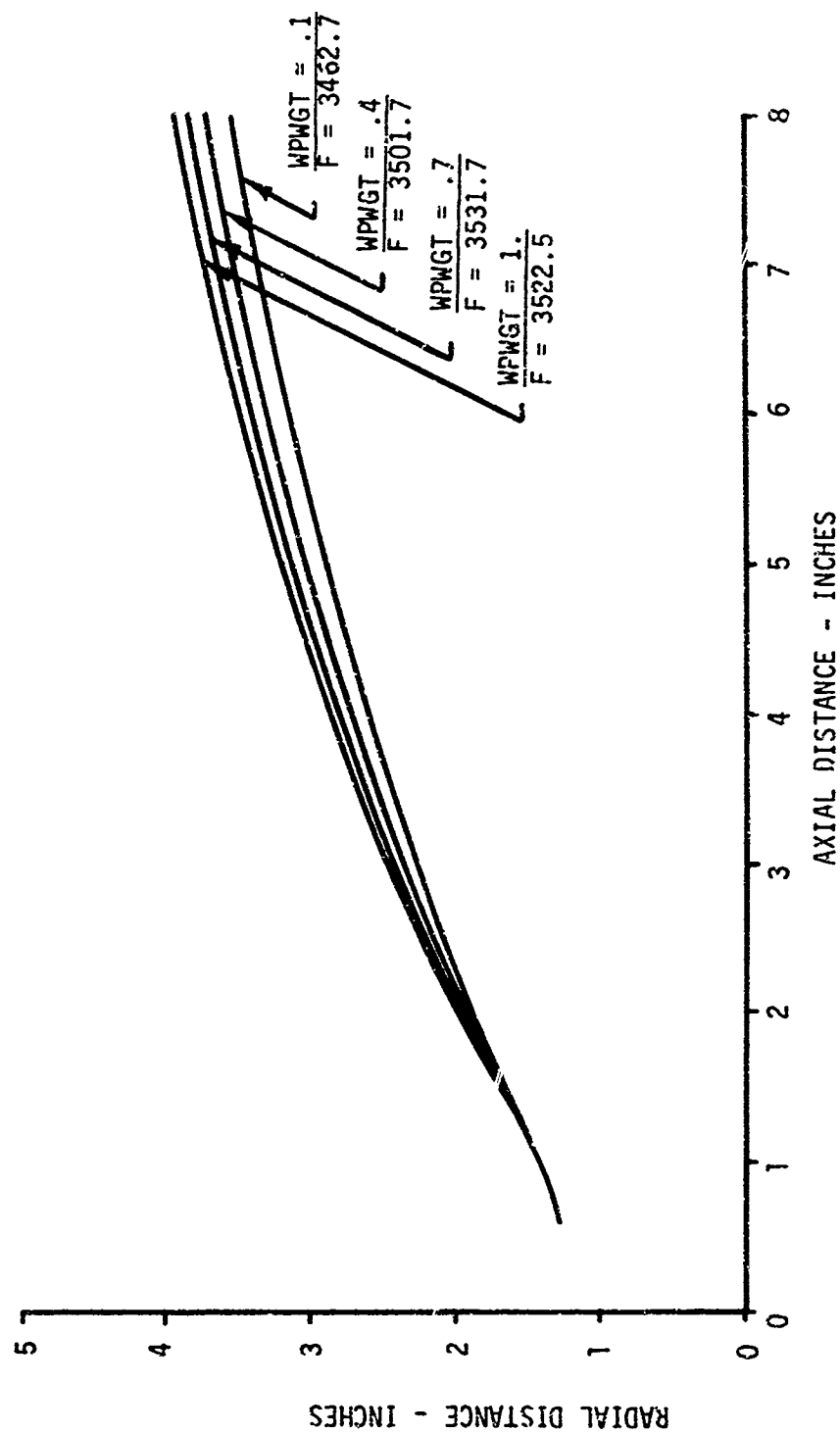


FIGURE 7. VARIATION OF PARTICLE MASS TO GAS MASS RATIO

is due to a combination of drag and heat transfer effects. The transfer of energy between the particles and the gas also results in increased thrust. This study did not consider changes in the combustion properties due to change in composition.

#### 5. VARIATION OF INLET ANGLE

When the inlet angle was changed, using the inlet angles of  $12^\circ$ ,  $30^\circ$  and  $48^\circ$ , it was found that the optimum nozzle contour was the same for all three cases. However, the limiting particle streamline was altered as shown in Figure 8, and the thrust value was affected by the opportunity for energy exchange between the particles and the gas. A 9.6 inch nozzle was specified, again using 4 micron particles and  $WPWGT = 0.4$ . The thrust increased as the particles occupied greater portions of the nozzles, permitting more effective energy transfer. This indicates that the nozzle inlet contour should be designed to bring the limiting particle streamline near the end of the nozzle contour while avoiding impingement.

#### 6. VARIATION OF THE DRAG AND HEAT TRANSFER COEFFICIENTS

Parametric studies were conducted to determine the effect of inaccuracies in the empirical drag and heat transfer coefficients used in the program. The parametric studies were performed using a nozzle length of 9.6 inches,  $WPWGT = 0.4$ , 4 micron particle size and  $NILP = 12$ . The inlet angle was 30 degrees.

The drag coefficients and heat transfer coefficients are calculated from tabular data. The tabular data give empirical ratios of the coefficients for specific values of Reynolds numbers to the coefficients for Stokes flow regime. The drag coefficient and heat transfer coefficient tables used in the program are the ones used by Kliegel and Nickerson (14),

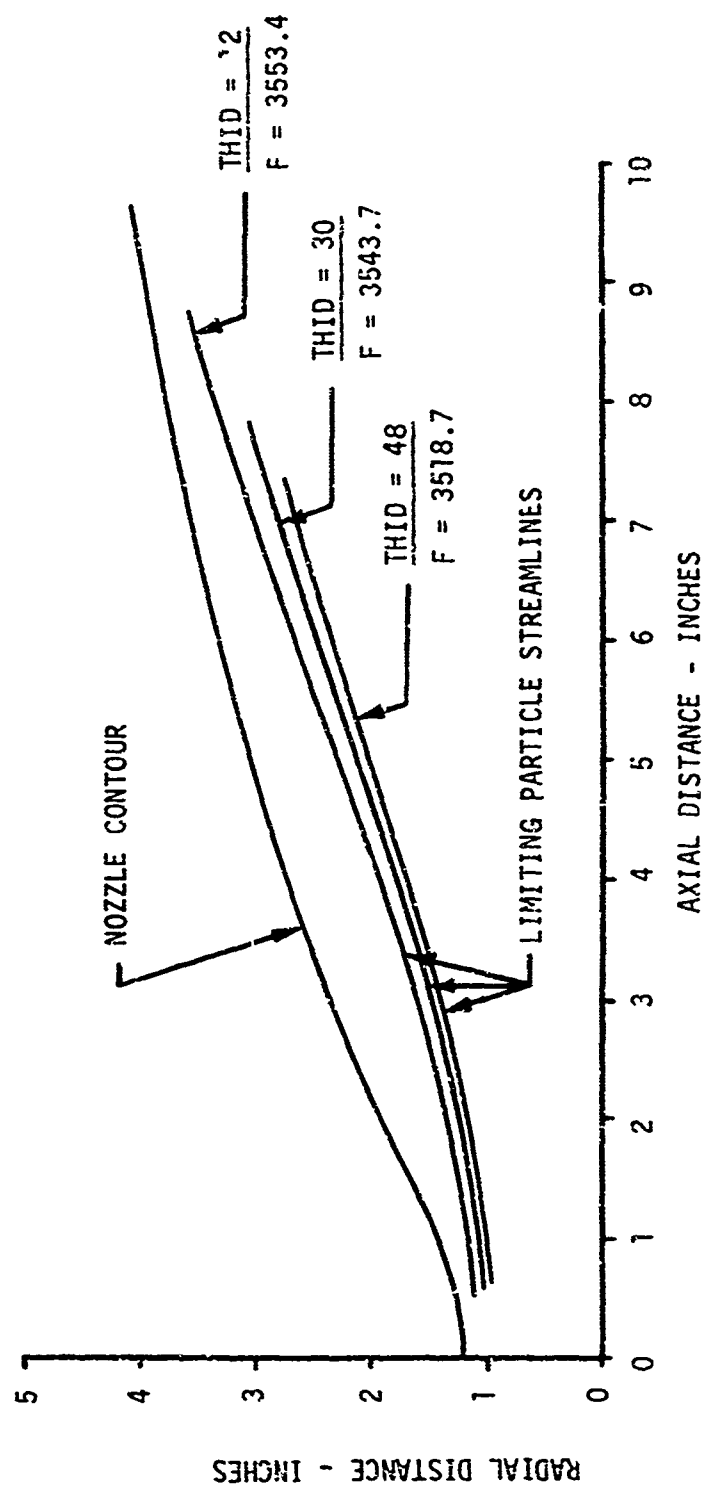


FIGURE 8. INLET ANGLE EFFECTS

but can be changed easily by the program user if desired. Rarefaction corrections are applied to the drag and heat transfer coefficients calculated from the tables.

Figure 9 compares the effect of increasing the drag coefficient by a factor of 3 and decreasing the drag coefficient by a factor of 3 relative to the standard case. The optimized nozzle contours were the same for all three cases, but the limiting particle streamline was affected substantially. The case with the higher drag coefficient results in greater thrust. Since the particles occupy a greater portion of the nozzle, the heat transfer is more effective.

Figure 10 compares the effect of varying the heat transfer coefficient. The larger heat transfer coefficient results in larger computed thrust values and nozzle contours with greater expansion ratios. A ninefold increase in heat transfer coefficient increases the thrust 0.5 percent. Particle impingement is not of concern since the limiting particle streamline moves in the same direction and by approximately the same distance as the nozzle contour moves.

## 7. VARIATION OF THE THROAT RADIUS OF CURVATURE

The throat radius of curvature (RRT) is expressed in throat radii. The throat radius of curvature parametric study compares results with throat radii of curvature of 1.5 throat radii, 2.5 throat radii and 3.5 throat radii. An inlet angle of  $30^\circ$  and nozzle length of 8 inches were used. The computed thrust values are nearly the same although the nozzle contours and expansion ratios vary. (See Figure 11). The supersonic portion of the nozzle contours are very similar, however, if they are translated in the axial direction a sufficient distance to compensate for the variation in throat length.

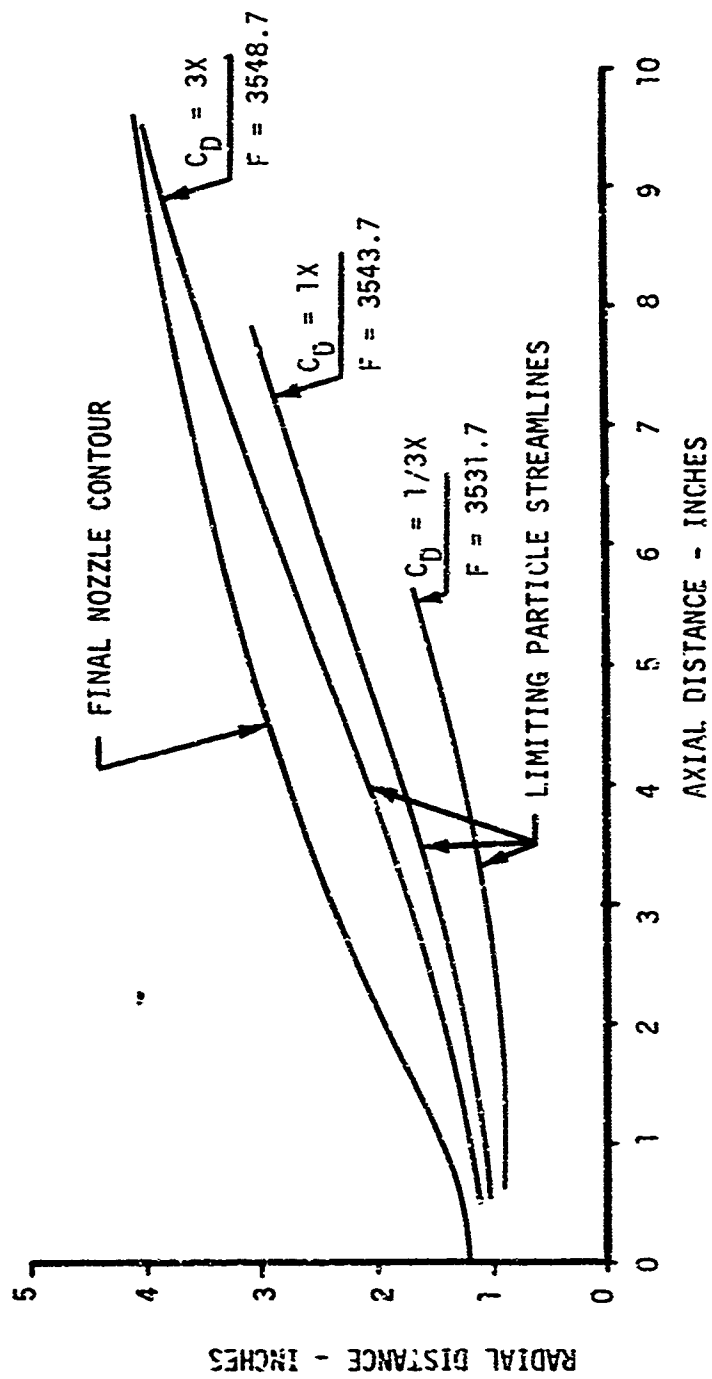


FIGURE 9. EFFECT OF DRAG COEFFICIENT VARIATION

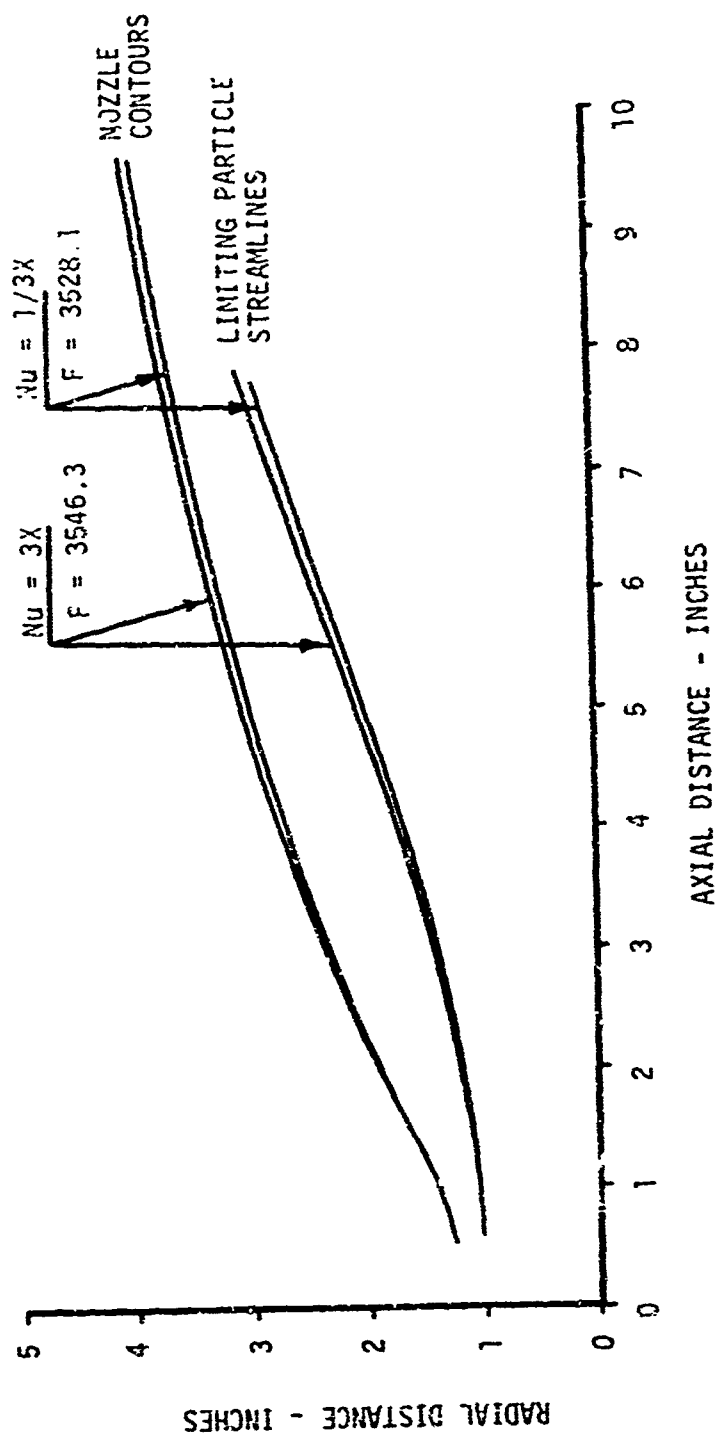


FIGURE 10. EFFECT OF HEAT TRANSFER COEFFICIENT VARIATION

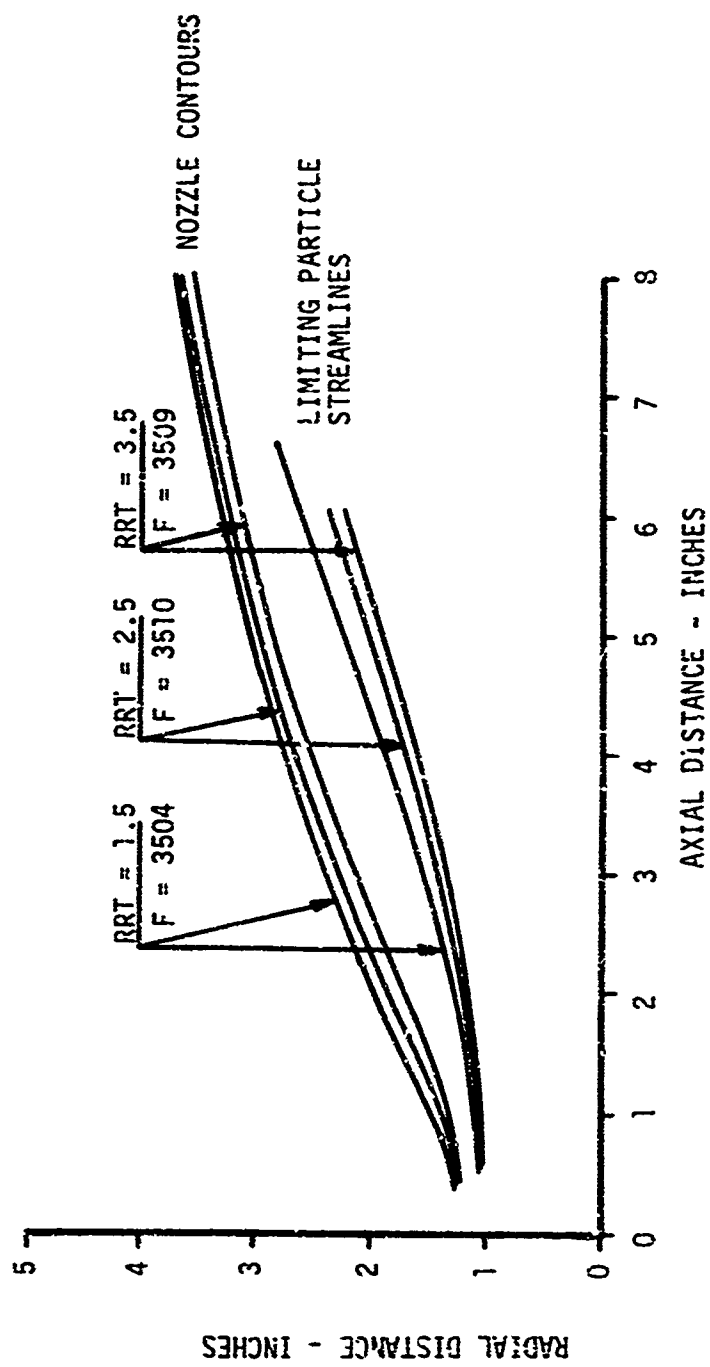


FIGURE 11. EFFECT OF THROAT RADIUS OF CURVATURE

The limiting particle streamline was also affected by the change in the throat radius of curvature. With larger values for RRT, the curvature of the wall at the throat region is more gradual, permitting the particles to accelerate more in the axial direction prior to being subjected to vertical drag forces. The resulting momentum provides a greater separation between the nozzle wall and the limiting particle streamline.

This parametric study indicates that it may be advantageous to use the larger throat radius of curvature, since thrust is not lost, particle impingement with the wall is avoided, and there is a possibility that the nozzle weight could be reduced.

#### 8. NOZZLE SCALING

Since two-phase flow is dissipative, scaling of the results of one design to provide a nozzle of greater or less thrust is not applicable. A parametric study was conducted to illustrate the effects of scaling. An inlet angle of  $45^\circ$  and a throat radius of curvature of 3 throat radii were used for each case. The nominal case was a 4.8 inch long nozzle with throat radius of 0.6 inch. Additional cases were two times, four times and eight times the size of the nominal case nozzle.

The maximum thrust nozzle contours for the larger nozzles result in a greater expansion ratio. (See Figure 12). A more marked effect, however, is seen in the locations of the limiting particle streamlines. The location of these streamlines may dictate changes in the fixed portion of the nozzle in order to prevent impingement of particles on the nozzle contour or to increase the region in which energy can be transferred from the particles to the gas.

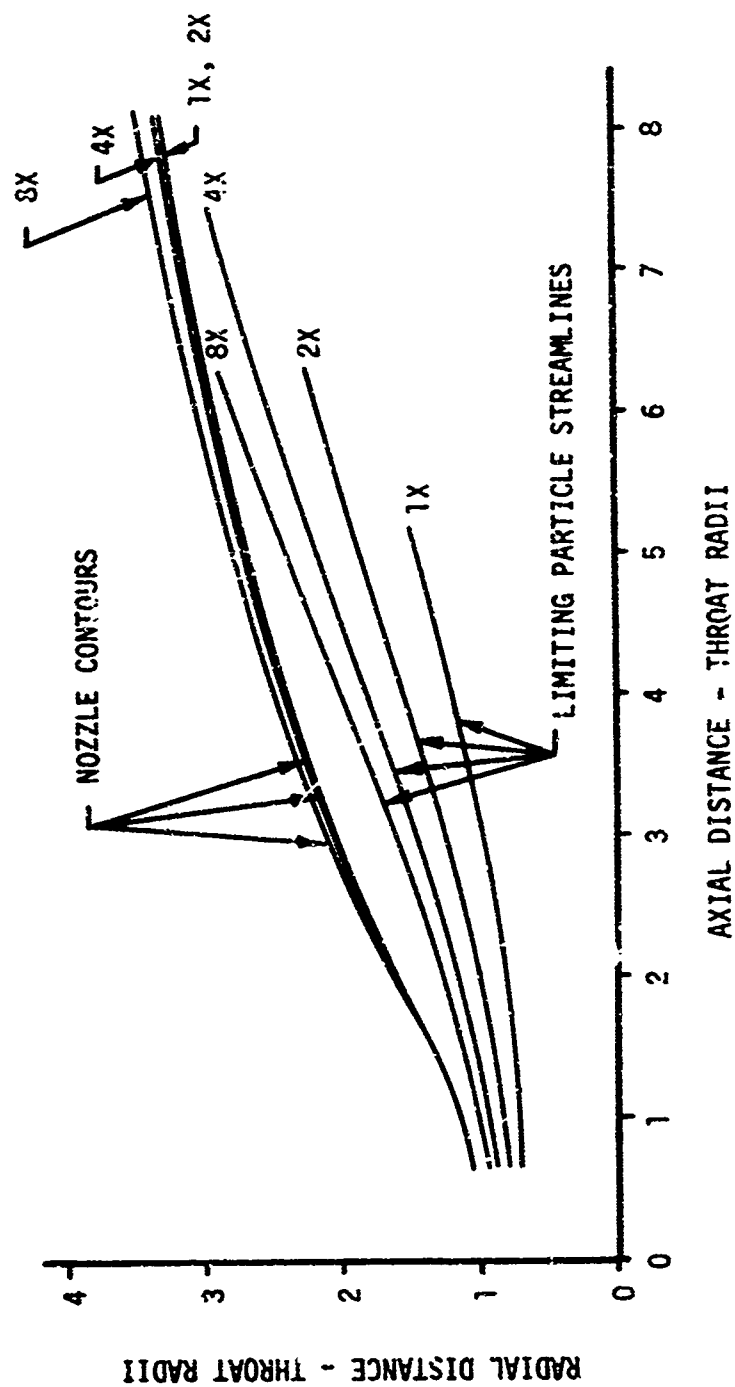


FIGURE 12. EFFECT OF SCALING

The calculated thrust for each of the final contours is shown in Table IV. If scaling of the nozzles and the thrust were applicable, the thrust would increase as the square of the increase in size. The results show that the thrust increase is slightly higher than direct scaling would indicate.

TABLE IV  
THRUST EVALUATION FOR NOZZLE SCALING

NOZZLE SIZE	THRUST	THRUST RATIO
1X	883.4	1.000
2X	3543.1	4.011
4X	14223.1	16.100
8X	57208.4	64.759

## SECTION V

### CONCLUSIONS

A formulation of the maximum thrust axisymmetric gas-particle nozzle problem was presented. A computer program was developed based on the optimization analysis. This computer program was used to conduct several parametric studies designed to determine the effect of various design parameters on the nozzle shape, limiting particle streamlines, and thrust of optimum nozzles.

The computer design program can be used either for analysis of nozzle flow or for design of the maximum thrust nozzle contour. Analysis of flow fields can be performed with four discrete particle sizes while the design of maximum thrust nozzles is limited to one particle size.

The results of several parametric studies were presented. The conclusions based on these studies include:

1. The change in nozzle contours as mesh size changes is negligible and the change in value of computed thrust is small. However, the mesh size does affect computer run time significantly.
2. The effect of particle size on the final nozzle contour was insignificant except for small particles whose limiting particle streamline lies near the nozzle contour, thus causing numerical scheme errors.
3. The ratio of the mass rate of flow of particles to the mass rate of flow of gas has a significant effect on both the final nozzle contour and the thrust. Higher concentrations of particles require a

greater expansion ratio to develop the maximum thrust and develop greater thrust.

4. Variation of the inlet angle to the nozzle throat does not appreciably affect the final nozzle contour, but does affect the limiting particle streamline and the thrust. Smaller inlet angles result in particles occupying a greater portion of the nozzle and a greater thrust.

5. Increasing the values of the drag coefficient does not appreciably affect the nozzle contour, but increases the portion of the nozzle which contains particles and increases the thrust.

6. Increasing the heat transfer coefficient increases the expansion ratio of the final nozzle contour, increases the portion of the nozzle which contains particles, and increases thrust.

7. Increasing the throat radius of curvature decreases the nozzle diameter but does not affect the thrust significantly. The increased throat radius of curvature results in greater separation between the limiting particle streamline and the nozzle contour.

## APPENDIX I

### DERIVATION OF THE EULER EQUATIONS

The extremal problem for the gas-particle nozzle optimization problem is given by the equation

$$I = \int_C^A H_1 dx + \iint_{ABC} \sum_{i=1}^8 h_i L_i dy dx \quad (91)$$

where

$$H_1 = (p - p_0) \eta \eta' + C_1 \xi + C_2 \eta \phi (u \eta' - v) \quad (31)$$

$$\begin{aligned} H_2 = & h_1 [y \rho u_x + y u \rho_x + y \rho v_y + y v \rho_y + \rho v] + \\ & + h_2 [\rho u u_x + \rho v u_y + p_x + A \rho_p (u - u_p)] + \\ & + h_3 [\rho u v_x + \rho v v_y + p_y + A \rho_p (v - v_p)] + \\ & + h_4 [u p_x + v p_y - a^2 u \rho_x - a^2 v \rho_y - A B \rho_p] + \\ & + h_5 [y \rho_p (u_p)_x + y u_p (\rho_p)_x + y \rho_p (v_p)_y + y v_p (\rho_p)_y + \rho_p v_p] + \\ & + h_6 [\rho_p u_p (u_p)_x + \rho_p v_p (u_p)_y - \rho_p A (u - u_p)] + \\ & + h_7 [\rho_p u_p (v_p)_x + \rho_p v_p (v_p)_y - \rho_p A (v - v_p)] + \\ & + h_8 [\rho_p u_p (h_p)_x + \rho_p v_p (h_p)_y - \frac{2}{3} A C \rho_p (T - T_p)] \end{aligned} \quad (92)$$

The functional,  $I$ , reaches a maximum when the maximum thrust nozzle design has been achieved. Under these conditions, the functional remains constant as minute changes are made in each of the dependent variables

$u, v, \rho, p, u_p, v_p, \rho_p$  and  $h_p$  independently of the others. It is possible then to take variations by setting the functional equal to the same functional with one of the dependent variables incremented an infinitesimal amount. The Euler equation used in the calculus of variations technique is one method of taking these variations over the region being considered and results in a set of eight equations.

The general form of the Euler equation is given by Miele (17) as

$$\frac{\partial H_2}{\partial z_k} - \frac{\partial}{\partial x} \left( \frac{\partial H_2}{\partial p_k} \right) - \frac{\partial}{\partial y} \left( \frac{\partial H_2}{\partial q_k} \right) = 0 \quad (k = 1, 2, \dots, 8) \quad (33)$$

where  $z_k$  denotes the eight dependent variables  $u, v, \rho, p, u_p, v_p, \rho_p$  and  $h_p$ , and  $p_k$  and  $q_k$  are defined as

$$p_k = \frac{\partial z_k}{\partial x} \quad (93)$$

$$q_k = \frac{\partial z_k}{\partial y} \quad (94)$$

A and C are constants, and

$$B = (\gamma - 1) [(u - u_p)^2 + (v - v_p)^2] - \frac{2}{3} C (T - T_p) \quad (10)$$

$$T = \frac{p}{\rho R} \quad (14)$$

$$T_p = T_p^0 + \frac{1}{C_c} (h_p - h_p^0) \quad (15)$$

$$a^2 = \frac{\gamma p}{\rho} \quad (16)$$

$h_p^0$  and  $T_p^0$  represent the reference enthalpy and temperature respectively and  $C_c$  is the specific heat of the condensed phase.

The general Euler equation, when applied to equation (92) with  $z_k = u$ , yields

$$\begin{aligned}
 & - (h_1 y \rho)_x + h_1 y \rho_x + h_2 \rho u_x - (h_2 \rho u)_x - (h_2 \rho v)_y + \\
 & + h_2 A \rho_p + h_3 \rho v_x + h_4 p_x - h_4 a^2 \rho_x - h_4 A \rho_p (\gamma - 1) 2(u - u_p) - \\
 & - h_6 A \rho_p = 0
 \end{aligned} \tag{95}$$

Simplifying and grouping terms results in

$$\begin{aligned}
 & - y \rho (h_1)_x + h_2 \rho u_x - h_2 (\rho u_x + u \rho_x + \rho v_y + v \rho_y) - \\
 & - \rho u (h_2)_x - \rho v (h_2)_y + h_3 \rho v_x + h_4 (p_x - a^2 \rho_x) + \\
 & + A \rho_p [h_2 - h_4 (\gamma - 1) 2(u - u_p) - h_6] = 0
 \end{aligned} \tag{96}$$

Using the gas continuity equation and rearranging gives the result

$$\begin{aligned}
 & - h_2 u_x - h_3 v_x - h_4 \frac{1}{\rho} (\rho_x - a^2 \rho_x) + y (h_1)_x + u (h_2)_x + v (h_2)_y = \\
 & = h_2 \frac{v}{y} + A \frac{\rho_p}{\rho} [h_2 - h_4 2(\gamma - 1)(u - u_p) - h_6]
 \end{aligned} \tag{34}$$

Performing the same operations with  $z_k = v$  yields

$$\begin{aligned}
 & - (h_1 y \rho)_y + h_1 y \rho_y + h_1 \rho + h_2 \rho u_y - (h_3 \rho u)_x + \\
 & + h_3 \rho v_y - (h_3 \rho v)_y + h_3 A \rho_p + h_4 p_y - h_4 a^2 \rho_y - \\
 & - h_4 A \rho_p (\gamma - 1)(v - v_p) - h_7 A \rho_p = 0
 \end{aligned} \tag{97}$$

$$\begin{aligned}
 & - y \rho (h_1)_y + h_2 \rho u_y - h_3 [\rho u_x + u \rho_x + \rho v_y + v \rho_y] + \\
 & + h_3 \rho v_y - \rho u (h_3)_x - \rho v (h_3)_y + h_4 (p_y - a^2 \rho_y) + \\
 & + A \rho_p [h_3 - h_4 (\gamma - 1) 2(v - v_p) - h_7] = 0
 \end{aligned} \tag{98}$$

$$\begin{aligned}
& - h_2 u_y - h_3 v_y - h_4 \frac{1}{\rho} (p_y - a^2 \rho_y) + y(h_1)_y + u(h_3)_x + v(h_3)_y = \\
& = h_3 \frac{v}{y} + A \frac{\rho}{\rho} [h_3 - h_4^2 (\gamma-1) (v-v_p) - h_7] \quad (35)
\end{aligned}$$

For  $z_k = p$ , the following result is obtained.

$$\begin{aligned}
& - (h_2)_x - (h_3)_y - (h_4 u)_x - (h_4 v)_y - h_4 u \rho_x \frac{\partial a^2}{\partial p} - \\
& - h_4 v \rho_y \frac{\partial a^2}{\partial p} - h_4 A \rho_p \frac{\partial B}{\partial p} - h_8 \frac{2}{3} A C \rho_p \frac{\partial T}{\partial p} = 0 \quad (99)
\end{aligned}$$

The partial derivatives with respect to  $p$  can be evaluated as follows.

$$\frac{\partial a^2}{\partial p} = \frac{\partial}{\partial p} \left( \frac{\gamma p}{\rho} \right) = \frac{\gamma}{\rho} = \frac{a^2}{p} \quad (100)$$

$$\frac{\partial T}{\partial p} = \frac{\partial}{\partial p} \left( \frac{p}{\rho R} \right) = \frac{1}{\rho R} = \frac{T}{p} \quad (101)$$

$$\frac{\partial B}{\partial p} = - (\gamma-1) \frac{2}{3} C \frac{\partial T}{\partial p} = - \frac{2}{3} \frac{C}{\rho R} (\gamma-1) \quad (102)$$

When equations (100) through (102) are substituted into equation (99), the final result is

$$\begin{aligned}
& h_4 u_x + h_4 v_y + h_4 \frac{a^2}{p} (u \rho_x + v \rho_y) + (h_2)_x + (h_3)_y + u(h_4)_x + \\
& + v(h_4)_y = A \frac{\rho}{\rho} \frac{2}{3} \frac{C}{R} [(\gamma-1) h_4 - h_8] \quad (36)
\end{aligned}$$

For  $z_k = \rho$ , the following result is found.

$$\begin{aligned}
& h_1 y u_x - (h_1 y u)_x + h_1 y v_y - (h_1 y v)_y + h_1 v + \\
& + h_2 u u_x + h_2 v u_y + h_3 u v_x + h_3 v v_y + \\
& + (h_4 a^2 u)_x - h_4 u \rho_x \frac{\partial a^2}{\partial \rho} + (h_4 a^2 v)_y - h_4 v \rho_y \frac{\partial a^2}{\partial \rho} - \\
& - h_4 a \rho_p \frac{\partial B}{\partial \rho} - h_8 \frac{2}{3} A C \rho_p \frac{\partial T}{\partial \rho} = 0 \quad (103)
\end{aligned}$$

The following relationships are used to eliminate density derivatives.

$$\frac{\partial a^2}{\partial \rho} = \frac{\partial}{\partial \rho} \left( \frac{\gamma p}{\rho} \right) = - \frac{\gamma p}{\rho^2} = - \frac{a^2}{\rho} \quad (104)$$

$$\frac{\partial T}{\partial \rho} = \frac{\partial}{\partial \rho} \left( \frac{p}{\rho R} \right) = - \frac{p}{\rho^2 R} = - \frac{T}{\rho} \quad (105)$$

$$\frac{\partial B}{\partial \rho} = \frac{\partial}{\partial \rho} \left( - \frac{2}{3} (\gamma - 1) CT \right) = \frac{2}{3} \frac{CT}{\rho} (\gamma - 1) \quad (106)$$

Using the two system momentum equations and equations (104) to (106), and grouping terms yields

$$\begin{aligned} & - \gamma u(h_1)_x - \gamma v(h_1)_y - h_2 \frac{p_x}{\rho} - h_3 \frac{p_y}{\rho} + \\ & + a^2 [h_4 u_x + u(h_4)_x + h_4 v_y + v(h_4)_y] + \\ & + h_4 u \frac{\partial a^2}{\partial x} + h_4 u \rho_x \frac{a^2}{\rho} + h_4 v \frac{\partial a^2}{\partial y} + h_4 v \rho_y \frac{a^2}{\rho} = \\ & = A \frac{p}{\rho} \left\{ h_2 (u - u_p) + h_3 (v - v_p) + \frac{2}{3} CT [h_4 (\gamma - 1) - h_8] \right\} \end{aligned} \quad (107)$$

Substituting in the Euler equation for  $z_k = p$  and using

$$\frac{\partial a^2}{\partial x} = \frac{\partial}{\partial x} \left( \frac{\gamma p}{\rho} \right) = \frac{a^2 p_x}{\rho} - \frac{a^2 \rho_x}{\rho} \quad (108)$$

$$\frac{\partial a^2}{\partial y} = \frac{\partial}{\partial y} \left( \frac{\gamma p}{\rho} \right) = \frac{a^2 p_y}{\rho} - \frac{a^2 \rho_y}{\rho} \quad (109)$$

reduces the equation to

$$\begin{aligned} & - \gamma u(h_1)_x - \gamma v(h_1)_y - h_2 \frac{p_x}{\rho} - h_3 \frac{p_y}{\rho} + \\ & + h_4 \frac{a^2}{\rho} \left\{ u p_x + v p_y - a^2 (u \rho_x + v \rho_y) \right\} - \end{aligned}$$

$$\begin{aligned}
& - a^2(h_2)_x - a^2(h_3)_y = A \frac{\rho_p}{\rho} \{h_2(u-u_p) + h_3(v-v_p)\} - \\
& - A \frac{\rho_p}{\rho} (\gamma-1) \left\{ \frac{2}{3} CT[h_4(\gamma-1) - h_p] \right\} \quad (110)
\end{aligned}$$

Finally, using the system energy equation, equation (110) becomes

$$\begin{aligned}
& \frac{h_2}{\rho} \rho_x + \frac{h_3}{\rho} \rho_y + yu(h_1)_x + yv(h_1)_y + a^2(h_2)_x + a^2(h_3)_y = \\
& = A \frac{\rho_p}{\rho} \left\{ \frac{2}{3} (\gamma-1) CT[(\gamma-1)h_4 - h_8] + \gamma h_4^5 - h_2(u-u_p) - h_3(v-v_p) \right\} \quad (37)
\end{aligned}$$

For  $z_k = u_p$ ,

$$\begin{aligned}
& - h_2 A \rho_p - h_4 A \rho_p (B)_{u_p} - (h_5 y \rho_p)_x + h_5 y (\rho_p)_x + \\
& + h_6 \rho_p (u_p)_x - (h_6 \rho_p u_p)_x - (h_6 \rho_p v_p)_y + h_6 A \rho_p + \\
& + h_7 \rho_p (v_p)_x + h_8 \rho_p (h_p)_x = 0 \quad (111)
\end{aligned}$$

where

$$(B)_{u_p} = -(\gamma-1)2(u - u_p) \quad (112)$$

Rearranging and simplifying, equation (111) becomes

$$\begin{aligned}
& - y \rho_p (h_5)_x - \rho_p u_p (h_6)_x - \rho_p v_p (h_6)_y + h_6 \rho_p (u_p)_x \\
& - h_6 [\rho_p (u_p)_x + u_p (\rho_p)_x + \rho_p (v_p)_y + v_p (\rho_p)_y] + \\
& + h_7 \rho_p (v_p)_x + h_8 \rho_p (h_p)_x = A \rho_p [h_2 - h_4 2(\gamma-1)(u-u_p) - h_6] \quad (113)
\end{aligned}$$

Using the particle continuity equation, the final result becomes

$$\begin{aligned}
& h_6(u_p)_x + h_7(v_p)_x + h_8(h_p)_x - y(h_5)_x - u_p(h_6)_x - v_p(h_5)_y = \\
& = A \left\{ h_2 - h_4 2(\gamma-1)(u-u_p) - h_6 \right\} - h_6 \frac{v_p}{y} \quad (38)
\end{aligned}$$

For  $z_k = v_p$ ,

$$\begin{aligned}
 & -h_3 A \rho_p - h_4 A \rho_p (B)_{v_p} - (h_5 y \rho_p)_y + h_5 y (\rho_p)_y + h_5 \rho_p + \\
 & + h_6 (u_p)_y - (h_7 \rho_p u_p)_x - (h_7 \rho_p v_p)_y + h_7 \rho_p (v_p)_y + h_7 A \rho_p + \\
 & \rho_p (h_p)_y = 0
 \end{aligned} \quad (114)$$

where

$$(B)_{v_p} = -(\gamma-1)2(v-v_p) \quad (115)$$

Simplifying, rearranging, and substituting the particle continuity equation in the same manner as for  $z_k = u_p$  yields

$$\begin{aligned}
 & h_6 (u_p)_y + h_7 (v_p)_y + h_8 (h_p)_y - y (h_5)_y - u_p (h_7)_x - v_p (h_7)_y = \\
 & = A \left\{ h_3 - h_4^2 (\gamma-1) (v-v_p) - h_7 \right\} - h_7 \frac{v_p}{y}
 \end{aligned} \quad (39)$$

For  $z_k = h_p$ ,

$$-h_4 A \rho_p (B)_{h_p} - (h_8 \rho_p u_p)_x - (h_8 \rho_p v_p)_y + h_8 \frac{2}{3} A C \rho_p (T_p)_{h_p} = 0 \quad (116)$$

where

$$(T_p)_{h_p} = \frac{\partial}{\partial h_p} \left( \frac{h_p}{C} \right) = \frac{1}{C} \quad (117)$$

$$(B)_{h_p} = \frac{\partial}{\partial h_p} \left[ (\gamma-1) \frac{2}{3} C T_p \right] = (\gamma-1) \frac{2}{3} \frac{C}{C} \quad (118)$$

Substituting in equations (117) and (118) and expanding terms yields

$$\begin{aligned}
 & \rho_p u_p (h_8)_x + \rho_p v_p (h_8)_y + h_8 [\rho_p (u_p)_x + u_p (\rho_p)_x + \rho_p (v_p)_y + v_p (\rho_p)_y] \\
 & + h_4 A \rho_p (\gamma-1) \frac{2}{3} \frac{C}{C} - h_8 \frac{2}{3} \rho_p \frac{AC}{C} = 0
 \end{aligned} \quad (119)$$

Substituting the particle continuity equation and simplifying results in

$$u_p(h_8)_x + v_p(h_8)_y = \frac{2}{3} \frac{AC}{C_c} \left\{ h_8 - (\gamma-1)h_4 \right\} + h_8 \frac{v_p}{y} \quad (40)$$

For  $z_k = p_p$ ,

$$\begin{aligned} h_2 A(u-u_p) + h_3 A(v-v_p) - h_4 AB + h_5 y(u_p)_x - \\ - (h_5 y u_p)_x + h_5 y (v_p)_y - (h_5 y v_p)_y + h_5 v_p = 0 \end{aligned} \quad (120)$$

which reduces to

$$y \left\{ u_p(h_5)_x + v_p(h_5)_y \right\} = A \left\{ h_2(u-u_p) + h_3(v-v_p) - h_4 B \right\} \quad (41)$$

## APPENDIX II

### CHARACTERISTIC AND COMPATIBILITY EQUATIONS

#### 1. GENERAL

The method of characteristics is frequently used to simplify the numeric calculations in supersonic flow fields, where the governing differential equations are hyperbolic. In this study, the governing differential equations are a system of hyperbolic, quasi-linear, non-homogeneous, partial differential equations of the first order as functions of two variables. A quasi-linear partial differential equation of the first order is defined as one which is non-linear in the dependent variables but linear in the first partial derivatives of the dependent variables.

The method of characteristics develops compatibility equations which express the dependent variables in terms of total derivatives rather than partial derivatives and the characteristic directions along which the compatibility equations apply. This system of equations is equivalent to the original set of equations and is convenient to use in a finite difference form. The characteristic and compatibility equations can be developed by use of determinants. However, the solution of the determinants is generally complex and an alternate method of obtaining the characteristic and compatibility equations is employed here.

The sixteen equations which are treated by the method of characteristics consist of the eight basic flow equations and the eight Euler equations. These equations are rewritten here for convenience.

$$L_1 = \rho u_x + \rho v_y + u \rho_x + v \rho_y + \frac{\rho v}{y} = 0 \quad (121)$$

$$L_2 = \rho u u_x + \rho v u_y + p_x + A \rho_p (u - u_p) = 0 \quad (122)$$

$$L_3 = \rho u v_x + \rho v v_y + p_y + A \rho_p (v - v_p) = 0 \quad (123)$$

$$L_4 = u p_x + v p_y - a^2 u \rho_x - a^2 v \rho_y - A B \rho_p = 0 \quad (124)$$

$$L_5 = \rho_p (u_p)_x + \rho_p (v_p)_y + u_p (\rho_p)_x + v_p (\rho_p)_y + \frac{\rho_p v_p}{y} = 0 \quad (125)$$

$$L_6 = \rho_p u_p (u_p)_x + \rho_p v_p (u_p)_y - A \rho_p (u - u_p) = 0 \quad (126)$$

$$L_7 = \rho_p u_p (v_p)_x + \rho_p v_p (v_p)_y - A \rho_p (v - v_p) = 0 \quad (127)$$

$$L_8 = \rho_p u_p (h_p)_x + \rho_p v_p (h_p)_y - \frac{2}{3} A C (T - T_p) = 0 \quad (128)$$

$$L_9 = -h_2 u_x - h_3 v_x - h_4 \frac{1}{\rho} p_x + h_4 \frac{a^2}{\rho} \rho_x + y (h_1)_x + \\ + u (h_2)_x + v (h_2)_y - K_1 = 0 \quad (129)$$

$$L_{10} = -h_2 u_y - h_3 v_y - h_4 \frac{1}{\rho} p_y + h_4 \frac{a^2}{\rho} \rho_y + y (h_1)_y + \\ + u (h_3)_x + v (h_3)_y - K_2 = 0 \quad (130)$$

$$L_{11} = h_4 u_x + h_4 v_y + h_4 \frac{a^2 u}{\rho} \rho_x + h_4 \frac{a^2 v}{\rho} \rho_y + (h_2)_x + \\ + (h_3)_y + u (h_4)_x + v (h_4)_y - K_3 = 0 \quad (131)$$

$$L_{12} = h_2 \frac{1}{\rho} p_x + h_3 \frac{1}{\rho} p_y + yu(h_1)_x + yv(h_1)_y + \\ + a^2(h_2)_x + a^2(h_3)_y - K_4 = 0 \quad (132)$$

$$L_{13} = h_6(u_p)_x + h_7(v_p)_x + h_8(h_p)_x - y(h_5)_x - \\ - u_p(h_6)_x - v_p(h_6)_y - K_5 = 0 \quad (133)$$

$$L_{14} = h_6(u_p)_y + h_7(v_p)_y + h_8(h_p)_y - y(h_5)_y - \\ - u_p(h_7)_x - v_p(h_7)_y - K_6 = 0 \quad (134)$$

$$L_{15} = u_p(h_8)_x + v_p(h_8)_y - K_7 = 0 \quad (135)$$

$$L_{16} = u_p(h_5)_x + v_p(h_5)_y - K_8 = 0 \quad (136)$$

where A, B and C are as previously defined in equations (9), (10) and (11), and

$$K_1 = h_2 \frac{v}{y} + A \frac{\rho_p}{\rho} \left\{ h_2 - h_4^2 (\gamma-1)(u-u_p) - h_6 \right\} \quad (137)$$

$$K_2 = h_3 \frac{v}{y} + A \frac{\rho_p}{\rho} \left\{ h_3 - h_4^2 (\gamma-1)(v-v_p) - h_7 \right\} \quad (138)$$

$$K_3 = A \frac{\rho_p}{\rho} \frac{2}{3} \frac{C}{R} \left\{ h_4 (\gamma-1) - h_8 \right\} \quad (139)$$

$$K_4 = A \frac{\rho_p}{\rho} \left\{ \frac{2}{3} (\gamma-1) CT [h_4(\gamma-1) - h_8] - \gamma h_4 B - \right. \\ \left. - h_2(u-u_p) - h_3(v-v_p) \right\} \quad (140)$$

$$K_5 = A \left\{ h_2 - h_4^2 (\gamma-1)(u-u_p) - h_6 \right\} - h_6 \frac{v_p}{y} \quad (141)$$

$$K_6 = A \left\{ h_3 - h_4^2 (\gamma-1)(v-v_p) - h_7 \right\} - h_7 \frac{v_p}{y} \quad (142)$$

$$K_7 = \frac{2}{3} A \frac{C}{C_c} \left\{ h_8 - h_4 (\gamma-1) \right\} + h_8 \frac{v_p}{y} \quad (143)$$

$$K_8 = A \left\{ h_2(u-u_p) + h_3(v-v_p) - h_4 B \right\} \quad (144)$$

It would be desirable to separate the development of method of characteristic equations into the flow field analysis portion involving  $L_1$  through  $L_8$  and the optimization portion involving  $L_9$  through  $L_{16}$  since the flow field analysis does not depend on whether optimization is performed. However, the presence of partial derivatives of the flow properties in  $L_9$  through  $L_{16}$  dictate against this approach. In reviewing the equations, it is noted, however, that  $L_1$  through  $L_4$  and  $L_9$  through  $L_{12}$  do not contain partial derivatives of particle properties or multipliers  $h_5$  through  $h_8$ . Also,  $L_5$  through  $L_8$  and  $L_{13}$  through  $L_{16}$  do not contain partial derivatives of gas properties or multipliers  $h_1$  through  $h_4$ . Thus the method of characteristics application may be simplified by dividing the problem into two segments, the gas property and associated multiplier equations and the particle property and associated multiplier equations.

## 2. GAS PROPERTY AND ASSOCIATED MULTIPLIER EQUATIONS

A differential operator is defined using arbitrary functions designated by  $\sigma$ 's as multipliers as follows:

$$L = \sigma_1 L_1 + \sigma_2 L_2 + \sigma_3 L_3 + \sigma_4 L_4 + \sigma_9 L_9 + \sigma_{10} L_{10} + \sigma_{11} L_{11} + \sigma_{12} L_{12} = 0 \quad (145)$$

By grouping partial differential terms, this equation can be rewritten

$$L = A \left\{ u_x + \frac{B}{A} u_y \right\} + C \left\{ v_x + \frac{D}{C} v_y \right\} + E \left\{ p_x + \frac{F}{E} p_y \right\} + G \left\{ \rho_x + \frac{H}{G} \rho_y \right\} + I \left\{ (h_1)_x + \frac{J}{I} (h_1)_y \right\} + K \left\{ (h_2)_x + \frac{L}{K} (h_2)_y \right\} + M \left\{ (h_3)_x + \frac{N}{M} (h_3)_y \right\} + P \left\{ (h_4)_x + \frac{Q}{P} (h_4)_y \right\} + R = 0 \quad (146)$$

where the coefficients are

$$A = \rho \sigma_1 + \rho u \sigma_2 - h_2 \sigma_9 + h_4 \sigma_{11} \quad (147)$$

$$B = \rho v \sigma_2 - h_2 \sigma_{10} \quad (148)$$

$$C = \rho \sigma_3 - h_3 \sigma_9 \quad (149)$$

$$D = \rho \sigma_1 + \rho v \sigma_3 - h_3 \sigma_{10} + h_4 \sigma_{11} \quad (150)$$

$$E = \sigma_2 + u \sigma_4 - h_4 \frac{1}{\rho} \sigma_9 + h_2 \frac{1}{\rho} \sigma_{12} \quad (151)$$

$$F = \sigma_3 + v \sigma_4 - h_4 \frac{1}{\rho} \sigma_{10} + h_3 \frac{1}{\rho} \sigma_{12} \quad (152)$$

$$G = u \sigma_1 - a^2 u \sigma_4 + h_4 \frac{a^2}{\rho} \sigma_9 + h_4 \frac{a^2 u}{p} \sigma_{11} \quad (153)$$

$$H = v \sigma_1 - a^2 v \sigma_4 + h_4 \frac{a^2}{\rho} \sigma_{10} + h_4 \frac{a^2 v}{p} \sigma_{11} \quad (154)$$

$$I = y\sigma_9 + yu\sigma_{12} \quad (155)$$

$$J = y\sigma_{10} + yv\sigma_{12} \quad (156)$$

$$K = u\sigma_9 + \sigma_{11} + a^2\sigma_{12} \quad (157)$$

$$L = v\sigma_9 \quad (158)$$

$$M = u\sigma_{10} \quad (159)$$

$$N = v\sigma_{10} + \sigma_{11} + a^2\sigma_{12} \quad (160)$$

$$P = u\sigma_{11} \quad (161)$$

$$Q = v\sigma_{11} \quad (162)$$

$$R = \frac{\partial v}{\partial y} \sigma_1 + A\sigma_p (u-u_p) \sigma_2 + A\sigma_p (v-v_p) \sigma_3 - AB\sigma_p \sigma_4 - \\ - K_1\sigma_9 - K_2\sigma_{10} - K_3\sigma_{11} - K_4\sigma_{12} \quad (163)$$

if each of the ratios multiplying the partial derivatives with respect to  $y$  are equal to a value  $\lambda = dy/dx$ , the differential operator reduces to

$$L = Adu + Cdv + Edp + Gdp + Idh_1 + \\ + Kdh_2 + Mdh_3 + Pdh_4 + Rdx = 0 \quad (164)$$

which is the desired form and is called the general compatibility equation.

Making the ratios each equal to  $\lambda$  results in the series of equations

$$A\lambda - B = 0 \quad (165)$$

$$C\lambda - D = 0 \quad (166)$$

$$E\lambda - F = 0 \quad (167)$$

$$G\lambda - H = 0 \quad (168)$$

$$I\lambda - J = 0 \quad (169)$$

$$K\lambda - L = 0 \quad (170)$$

$$M\lambda - N = 0 \quad (171)$$

$$P\lambda - Q = 0 \quad (172)$$

These equations are rearranged to group the arbitrary multiplier terms as the unknowns.

$$\rho\lambda\sigma_1 + \rho(u\lambda - v)\sigma_2 - h_2\lambda\sigma_9 + h_2\sigma_{10} + h_4\lambda\sigma_{11} = 0 \quad (173)$$

$$-\rho\sigma_1 + \rho(u\lambda - v)\sigma_3 - h_3\lambda\sigma_9 + h_3\sigma_{10} - h_4\sigma_{11} = 0 \quad (174)$$

$$\lambda\sigma_2 - \sigma_3 + (u\lambda - v)\sigma_4 - h_4\frac{1}{\rho}\lambda\sigma_9 + h_4\frac{1}{\rho}\sigma_{10} + \frac{1}{\rho}(h_2\lambda - h_3)\sigma_{12} = 0 \quad (175)$$

$$(u\lambda - v)\sigma_1 - a^2(u\lambda - v)\sigma_4 + h_4\frac{a^2}{\rho}\lambda\sigma_9 - h_4\frac{a^2}{\rho}\sigma_{10} + h_4\frac{a^2}{\rho}(u\lambda - v)\sigma_{11} = 0 \quad (176)$$

$$y\lambda\sigma_9 - y\sigma_{10} + y(u\lambda - v)\sigma_{12} = 0 \quad (177)$$

$$(u\lambda - v)\sigma_9 + \lambda\sigma_{11} + a^2\lambda\sigma_{12} = 0 \quad (178)$$

$$(u\lambda - v)\sigma_{10} - \sigma_{11} - a^2\sigma_{12} = 0 \quad (179)$$

$$(u\lambda - v)\sigma_{11} = 0 \quad (180)$$

If this system of equations is to have a solution other than the trivial solution with the arbitrary multipliers equal to zero, the determinant of the coefficients must equal zero. The determinant is shown in Figure 13. Expanding the determinant results in

$\rho\lambda$	$\rho(u\lambda-v)$	0	$-h_2\lambda$	$h_2$	$h_4\lambda$	0
$-\rho$	0	$\rho(u\lambda-v)$	$-h_3\lambda$	$h_3$	$-h_4$	0
0	$\lambda$	-1	$-h_4\frac{1}{\rho}\lambda$	$h_4\frac{1}{\rho}$	0	$\frac{1}{\rho}(h_2\lambda-h_3)$
$(u\lambda-v)$	0	0	$h_4\frac{a^2}{\rho}\lambda$	$-h_4\frac{a^2}{\rho}$	$h_4\frac{a^2}{\rho}(u\lambda-v)$	0
0	0	0	$y\lambda$	$-y$	0	$y(u\lambda-v)$
0	0	0	$(u\lambda-v)$	0	$\lambda$	$a^2\lambda$
0	0	0	0	$(u\lambda-v)$	-1	$-a^2$
0	0	0	0	0	$(u\lambda-v)$	0

= 0

FIGURE 13 DETERMINANT FOR FINDING GAS CHARACTERISTIC EQUATIONS

$$(u\lambda - v)^4 \left\{ (u^2 - a^2)\lambda^2 - 2uv\lambda + (v^2 - a^2) \right\}^2 = 0 \quad (181)$$

This equation is now solved for  $\lambda$  to give the characteristic equations along which the compatibility equations will be valid.

$$\lambda = \frac{dy}{dx} = \frac{v}{u} \quad (42)$$

$$\lambda = \frac{dy}{dx} = \frac{uv \pm a^2 \sqrt{M^2 - 1}}{u^2 - a^2} \quad (182)$$

Equation (42) is repeated four times in the solution of the determinant, indicating that four compatibility equations will apply along this characteristic direction. Each of the equations represented by equation (182) is repeated twice, indicating we can expect two compatibility equations for each of these characteristic directions. For convenience, equation (182) is expressed in terms of the flow angle  $\theta$ , and the mach angle  $\alpha$ .

$$\lambda = \frac{dy}{dx} = \tan(\theta \pm \alpha) \quad (45)$$

Now that the characteristic equations are known, the compatibility equations are determined from the general compatibility equation, equation (164). First, the arbitrary multipliers in the coefficients must be determined or otherwise eliminated. This is accomplished by substituting each of the characteristic equations into equations (165) through (172). When  $\lambda = v/u$  is used, the following series of equations result:

$$\frac{v}{u} \sigma_1 - h_2 \frac{v}{u} \sigma_9 + h_2 \sigma_{10} + h_4 \frac{v}{u} \sigma_{11} = 0 \quad (183)$$

$$-\rho \sigma_1 - h_3 \frac{v}{u} \sigma_9 + h_3 \sigma_{10} - h_4 \sigma_{11} = 0 \quad (184)$$

$$\frac{v}{u} \sigma_2 - \sigma_3 - h_4 \frac{1}{\rho} \frac{v}{u} \sigma_9 + h_4 \frac{1}{\rho} \sigma_{10} + \frac{1}{\rho} (h_2 \frac{v}{u} - h_3) \sigma_{12} = 0 \quad (185)$$

$$h_4 \frac{a^2}{\rho} \frac{v}{u} \sigma_9 - h_4 \frac{a^2}{\rho} \sigma_{10} = 0 \quad (186)$$

$$\frac{v}{u} \sigma_9 - \sigma_{10} = 0 \quad (187)$$

$$\sigma_{11} + a^2 \sigma_{12} = 0 \quad (188)$$

$$\sigma_{11} + a^2 \sigma_{12} = 0 \quad (189)$$

$$0 = 0 \quad (190)$$

Only four independent equations result from this set.

$$\sigma_1 = h_4 \frac{a^2}{\rho} \sigma_{12} \quad (191)$$

$$\sigma_3 = \lambda \sigma_2 + \frac{1}{\rho} (h_2 \lambda - h_3) \sigma_{12} \quad (192)$$

$$\sigma_{10} = \lambda \sigma_9 \quad (193)$$

$$\sigma_{11} = -a^2 \sigma_{12} \quad (194)$$

Four  $\sigma$ 's must be taken as arbitrary. Since  $\sigma_4$  does not appear in the four independent equations, it is selected as one of the arbitrary  $\sigma$ 's.

The others selected are  $\sigma_2$ ,  $\sigma_9$  and  $\sigma_{12}$ .

Now the general compatibility is rewritten, grouping terms containing each of the four arbitrary  $\sigma$ 's together to yield

$$\begin{aligned} & \left\{ \rho u du + \rho v dv + dp + A \rho_p (u - u_p) dx + A \rho_p (v - v_p) dy \right\} \sigma_2 + \\ & + \left\{ u dp - a^2 u d\rho - A B \rho_p dx \right\} \sigma_4 + \\ & + \left\{ -h_2 du - h_3 dv - h_4 \frac{1}{\rho} dp + h_4 \frac{a^2}{\rho} d\rho + y dh_1 + \right. \end{aligned}$$

$$\begin{aligned}
& + u dh_2 + v dh_3 - K_1 dx - K_2 dy \} \sigma_9 + \\
& + \left\{ (v h_2 - u h_3) dv + h_2 \frac{1}{\rho} dp - u h_4 \frac{a^2}{\rho} (\gamma-1) d\rho + \right. \\
& + y u dh_1 - a^2 u dh_4 + (h_4 a^2 \frac{v}{y} + a^2 K_3 - K_4) dx + \\
& \left. + A \frac{\rho p}{\gamma} (v-v_p) (h_2 dy - h_3 dx) \right\} \sigma_{12} = 0
\end{aligned} \tag{195}$$

Since the  $\sigma$ 's are arbitrary, their coefficients must each equal zero, resulting in four compatibility equations which apply along the characteristic direction  $\lambda = v/u$ .

$$\rho u du + \rho v dv + dp = -A \rho_p \left\{ (u-u_p) dx + (v-v_p) dy \right\} \tag{18}$$

$$u dp - a^2 u d\rho = A B \rho_p dx \tag{19}$$

$$\begin{aligned}
& - h_2 du - h_3 dv - h_4 \frac{1}{\rho} dp + h_4 \frac{a^2}{\rho} d\rho + y dh_1 + \\
& + u dh_2 + v dh_3 - K_1 dx - K_2 dy = 0
\end{aligned} \tag{196}$$

$$\begin{aligned}
& (v h_2 - u h_3) dv + h_2 \frac{1}{\rho} dp - u h_4 \frac{a^2}{\rho} (\gamma-1) d\rho + \\
& + y u dh_1 - a^2 u dh_4 + (h_4 a^2 \frac{v}{y} + a^2 K_3 - K_4) dx + \\
& + A \frac{\rho p}{\gamma} (v-v_p) (h_2 dy - h_3 dx) = 0
\end{aligned} \tag{197}$$

Along the characteristic directions given by  $\lambda = \tan (\theta-\alpha)$ , the following equation is valid.

$$\lambda^2(u^2 - a^2) - 2uv\lambda + (v^2 - a^2) = 0 \tag{198}$$

The quantity  $u\lambda - v$  cannot be zero, therefore  $\sigma_{11}$  must be according to

equation (180). Then  $\sigma_9$  and  $\sigma_{10}$  can be found from equations (178) and (179).  $\sigma_9$  and  $\sigma_{10}$  are eliminated from the remaining equations and  $\sigma_1$  determined from equation (176). This is used to eliminate  $\sigma_1$  from equations (173) and (174). Finally, using equation (198) to reduce the results, the eight equations are reduced to

$$\sigma_2 = -\frac{\lambda a^2}{(u\lambda-v)} \sigma_4 - \frac{1}{\rho} \left\{ h_2 + \frac{\lambda a^2}{(u\lambda-v)} h_4 \right\} \sigma_{12} \quad (199)$$

$$\sigma_3 = \frac{a^2}{(u\lambda-v)} \sigma_4 + \frac{1}{\rho} \left\{ \frac{a^2}{(u\lambda-v)} h_4 - h_3 \right\} \sigma_{12} \quad (200)$$

$$-\sigma_2 \lambda + \sigma_3 = \sigma_4 (u\lambda-v) + \frac{1}{\rho} \left\{ (u\lambda-v) h_4 + h_2 \lambda - h_3 \right\} \sigma_{12} \quad (201)$$

$$\sigma_1 = a^2 \sigma_4 + \frac{1}{\rho} h_4 a^2 \sigma_{12} \quad (202)$$

$$\sigma_{12} \left\{ 0 \right\} = 0 \quad (203)$$

$$\sigma_9 = -\frac{a^2 \lambda}{(u\lambda-v)} \sigma_{12} \quad (204)$$

$$\sigma_{10} = \frac{a^2}{(u\lambda-v)} \sigma_{12} \quad (205)$$

$$\sigma_{11} = 0 \quad (206)$$

Equation (201) may be obtained by multiplying equation (199) by  $-\lambda$  and adding to equation (200). Thus, two of the above equations, (201) and (203) are not independent. Therefore, two of the  $\sigma$ 's must be arbitrary.  $\sigma_4$  and  $\sigma_{12}$  are selected. Substituting the six independent equations into the general compatibility equation and setting the coefficients of  $\sigma_4$  and  $\sigma_{12}$  to zero results in the following two equations.

$$\begin{aligned}
& \left\{ \rho a^2 - \frac{\rho u \lambda a^2}{u \lambda - v} \right\} du + \left\{ \frac{\rho u a^2}{u \lambda - v} \right\} dv + \left\{ -\frac{\lambda a^2}{u \lambda - v} + u \right\} dp + \\
& + \left\{ \frac{\rho a^2 v}{y} - A \rho_p \frac{\lambda a^2}{u \lambda - v} (u - u_p) + A \rho_p \frac{a^2}{u \lambda - v} (v - v_p) - \right. \\
& \left. - AB \rho_p \right\} dx = 0
\end{aligned} \quad (207)$$

$$\begin{aligned}
& \left\{ h_4 a^2 - u h_2 - \frac{u \lambda a^2}{u \lambda - v} h_4 + \frac{a^2 \lambda}{u \lambda - v} h_2 \right\} du + \\
& + \left\{ \frac{u a^2}{u \lambda - v} h_4 - u h_3 + \frac{a^2 \lambda}{u \lambda - v} h_3 \right\} dv + \left\{ \frac{a^2}{\rho} (u h_4 - \frac{a^2 \lambda}{u \lambda - v} h_4) \right\} dp + \\
& + \left\{ -y \frac{a^2 \lambda}{u \lambda - v} + u y \right\} dh_1 - \left\{ \frac{u a^2 \lambda}{u \lambda - v} - a^2 \right\} dh_2 + \left\{ \frac{u a^2}{u \lambda - v} \right\} dh_3 + \\
& + \left\{ \frac{v}{y} h_4 a^2 - A \frac{\rho_p}{\rho} (h_2 + \frac{\lambda a^2}{u \lambda - v} h_4) (u - u_p) + \right. \\
& + A \frac{\rho_p}{\rho} \left( \frac{a^2}{u \lambda - v} h_4 - h_3 \right) (v - v_p) + k_1 \frac{a^2 \lambda}{u \lambda - v} - \\
& \left. - k_2 \frac{a^2}{u \lambda - v} - k_4 \right\} dx = 0
\end{aligned} \quad (208)$$

After some manipulation including the use of equation (198) and the relationships

$$\frac{uv - \lambda(u^2 - a^2)}{a^2} = \pm \cot \alpha \quad (209)$$

$$\frac{a^2}{u^2 \lambda - uv - a^2 \lambda} = \mp \tan \alpha \quad (210)$$

the compatibility equations become

$$\begin{aligned}
& a^2 [v du - u dv] \pm \frac{a^2}{\rho} \cot \alpha dp = \frac{a^2 v}{y} (udy - vdx) - \\
& - A \frac{\rho_p}{\rho} \left\{ B(udy - vdx) + a^2 [(u - u_p)dy - (v - v_p)dx] \right\}
\end{aligned} \quad (21)$$

$$\begin{aligned}
& h_2 du + h_3 dv + \frac{1}{\rho} h_4 (dp - a^2 d\rho) - y dh_1 + \tan \alpha (v dh_2 - u dh_3) = \\
& = \pm \tan \alpha \left\{ h_3 \frac{v}{y} dx + A \frac{\rho}{\rho} [h_3 - h_4^2 (\gamma - 1) (v - v_p) - h_7] dx - \right. \\
& \quad - h_2 \frac{v}{y} dy - A \frac{\rho}{\rho} [h_2 - h_4^2 (\gamma - 1) (u - u_p) - h_6] dy + \\
& \quad \left. + \frac{1}{2} (udy - vdx) A \frac{\rho}{\rho} (\gamma - 1) \left[ \frac{2}{3} CT \left\{ (\gamma - 1) h_4 - h_8 \right\} + h_4 B \right] \right\} \\
& \hspace{15em} (46)
\end{aligned}$$

These equations represent the four equations which apply along the Mach lines.

### 3. PARTICLE PROPERTY AND ASSOCIATED MULTIPLIER EQUATIONS

The differential operator in the case of particle properties and associated multipliers is

$$L = \sigma_5 L_5 + \sigma_6 L_6 + \sigma_7 L_7 + \sigma_8 L_8 + \sigma_{13} L_{13} + \sigma_{14} L_{14} + \sigma_{15} L_{15} + \sigma_{16} L_{16} \quad (211)$$

or, regrouping by partial differential terms,

$$\begin{aligned}
L = & A \left\{ (u_p)_x + \frac{B}{A} (u_p)_y \right\} + C \left\{ (v_p)_x + \frac{D}{C} (v_p)_y \right\} + \\
& + E \left\{ (h_p)_x + \frac{F}{E} (h_p)_y \right\} + G \left\{ (\rho_p)_x + \frac{H}{G} (\rho_p)_y \right\} + \\
& + I \left\{ (h_5)_x + \frac{J}{I} (h_5)_y \right\} + K \left\{ (h_6)_x + \frac{L}{K} (h_6)_y \right\} + \\
& + M \left\{ (h_7)_x + \frac{N}{M} (h_7)_y \right\} + P \left\{ (h_8)_x + \frac{Q}{P} (h_8)_y \right\} + R = 0 \quad (212)
\end{aligned}$$

where the coefficients are

$$A = \rho_p \sigma_5 + \rho_p u_p \sigma_6 + h_6 \sigma_{13} \quad (213)$$

$$B = \rho_p v_p \sigma_6 + h_6 \sigma_{14} \quad (214)$$

$$C = \rho_p u_p \sigma_7 + h_7 \sigma_{13} \quad (215)$$

$$D = \rho_p \sigma_5 + \rho_p v_p \sigma_7 + h_7 \sigma_{14} \quad (216)$$

$$E = \rho_p u_p \sigma_8 + h_8 \sigma_{13} \quad (217)$$

$$F = \rho_p v_p \sigma_8 + h_8 \sigma_{14} \quad (218)$$

$$G = u_p \sigma_5 \quad (219)$$

$$H = v_p \sigma_5 \quad (220)$$

$$I = -y \sigma_{13} + u_p \sigma_{16} \quad (221)$$

$$J = -y \sigma_{14} + v_p \sigma_{16} \quad (222)$$

$$K = -u_p \sigma_{13} \quad (223)$$

$$L = -v_p \sigma_{13} \quad (224)$$

$$M = -u_p \sigma_{14} \quad (225)$$

$$N = -v_p \sigma_{14} \quad (226)$$

$$P = u_p \sigma_{15} \quad (227)$$

$$Q = v_p \sigma_{15} \quad (228)$$

$$R = \frac{\rho_p u_p}{y} \sigma_5 - A \rho_p (u - u_p) \sigma_6 - A c_p (v - v_p) \sigma_7 - \frac{2}{3} A C (T - T_p) \sigma_8 -$$

$$- K_5 \sigma_{13} - K_6 \sigma_{14} - K_7 \sigma_{15} - K_8 \sigma_{16} \quad (229)$$

The general compatibility equation is

$$L = Adu_p + Cdv_p + Edh_p + Gh\rho_p + Idh_5 + Kdh_6 + Mdh_7 + Pd h_8 + Rdx = 0 \quad (230)$$

Setting the ratios which multiply the partial derivatives with respect to  $y$  equal to  $\lambda$ , and grouping terms by the  $\sigma$ 's results in

$$\rho_p \lambda \sigma_5 + \rho_p (u_p \lambda - v_p) \sigma_6 + h_6 \lambda \sigma_{13} - h_6 \sigma_{14} = 0 \quad (231)$$

$$-\rho_p \sigma_5 + \rho_p (u_p \lambda - v_p) \sigma_7 + h_7 \lambda \sigma_{13} - h_7 \sigma_{14} = 0 \quad (232)$$

$$\rho_p (u_p \lambda - v_p) \sigma_8 + h_8 \lambda \sigma_{13} - h_8 \sigma_{14} = 0 \quad (233)$$

$$(u_p \lambda - v_p) \sigma_5 = 0 \quad (234)$$

$$-y \lambda \sigma_{13} + y \sigma_{14} + (u_p \lambda - v_p) \sigma_{16} = 0 \quad (235)$$

$$- (u_p \lambda - v_p) \sigma_{13} = 0 \quad (236)$$

$$- (u_p \lambda - v_p) \sigma_{14} = 0 \quad (237)$$

$$(u_p \lambda - v_p) \sigma_{15} = 0 \quad (238)$$

The determinant of the coefficients is presented in Figure 14. Expansion of the determinant results in

$$(u_p \lambda - v_p)^8 = 0 \quad (239)$$

$\rho_p \lambda$	$\rho_p(u_p \lambda - v_p)$	0	0	$h_6 \lambda$	$-h_6$	0	0
$-\rho_p$	0	$\rho_p(u_p \lambda - v_p)$	0	$h_7 \lambda$	$-h_7$	0	0
0	0	0	$\rho_p(u_p \lambda - v_p)$	$h_8 \lambda$	$-h_8$	0	0
$(u_p \lambda - v_p)$	0	0	0	0	0	0	0
0	0	0	0	$-y \lambda$	y	0	$(u_p \lambda - v_p)$
0	0	0	0	$-(u_p \lambda - v_p)$	0	0	0
0	0	0	0	0	$-(u_p \lambda - v_p)$	0	0
0	0	0	0	0	0	$(u_p \lambda - v_p)$	0

= 0

FIGURE 14 DETERMINANT FOR FINDING PARTICLE CHARACTERISTIC EQUATIONS

Thus, the characteristic equation is

$$\lambda = \frac{dy}{dx} = \frac{v_p}{u_p} \quad (22)$$

and eight compatibility equations should apply along that direction.

Substituting the characteristic equation into equations (231} through (238) results in the following equations,

$$\rho_p \frac{v_p}{u_p} \sigma_5 + h_6 \frac{v_p}{u_p} \sigma_{13} - h_6 \sigma_{14} = 0 \quad (240)$$

$$-\rho_p \sigma_5 + h_7 \frac{v_p}{u_p} \sigma_{13} - h_7 \sigma_{14} = 0 \quad (241)$$

$$h_8 \frac{v_p}{u_p} \sigma_{13} - h_8 \sigma_{14} = 0 \quad (242)$$

$$\sigma_5 (0) = 0 \quad (243)$$

$$\frac{v_p}{u_p} \sigma_{13} - \sigma_{14} = 0 \quad (244)$$

$$\sigma_{13} (0) = 0 \quad (245)$$

$$\sigma_{14} (0) = 0 \quad (246)$$

$$\sigma_{15} (0) = 0 \quad (247)$$

which reduce to only two independent equations.

$$\sigma_5 = 0 \quad (248)$$

$$\sigma_{14} = \frac{v_p}{u_p} \sigma_{13} \quad (249)$$

Setting the coefficients of the arbitrary multipliers,  $\lambda_6, \lambda_7, \lambda_8, \lambda_{13}, \lambda_{15}$  and  $\lambda_{16}$ , in equation (230), the general compatibility equation for particle properties and associated multipliers, equal to zero results in the following compatibility equations along the particle streamline:

$$u_p du_p = A (u - u_p) dx \quad (23)$$

$$u_p dv_p = A (v - v_p) dx \quad (24)$$

$$u_p dh_p = \frac{2}{3} AC (T - T_p) dx \quad (25)$$

$$u_p dh_5 = A[h_2 (u - u_p) + h_3 (v - v_p) - h_4 B] dx \quad (48)$$

$$\begin{aligned} h_6 du_p + h_7 dv_p + h_8 dh_p - y dh_5 - u_p dh_6 - v_p dh_7 = \\ = A \left\{ h_2 - h_4 2(\gamma - 1) (u - u_p) - h_6 \right\} dx - h_6 \frac{v_p}{y} dx + \\ + A \left\{ h_3 - h_4 2(\gamma - 1) (v - v_p) - h_7 \right\} dy - h_7 \frac{v_p}{y} dy \end{aligned} \quad (49)$$

$$u_p dh_8 = \frac{2}{3} \frac{AC}{C_c} [h_8 - (\gamma - 1) h_4] dx + h_8 \frac{v_p}{y} dx \quad (50)$$

A deficiency of two compatibility equations exists. None of the equations have derivatives of the particle density function,  $\rho_p$ . This deficiency is corrected by the use of a numerical integration scheme to determine the  $\rho_p$ . The other deficiency prevents the calculation of the multipliers  $h_6$  and  $h_7$  since derivatives of these variables appear only in equation (49). This deficiency is corrected by using a numerical evaluation scheme to evaluate two of the Euler equations, (38) and (39), which permit writing them in a compatibility like form for the evaluation of  $h_6$  and  $h_7$  along particle streamlines. Equation (49) is not used, being replaced by the two compatibility like equations.

### APPENDIX III

#### THE CORNER CONDITION

When the end points of an extremum are allowed to vary, the variation must result in no change in the function,  $I$ , if the functional is at either a maximum or a minimum. In the calculus of variations, this restriction is expressed by the corner condition as given by Miele (17).

$$\Delta \left\{ H_1 - y' \frac{\partial H_1}{\partial v'} \right\} \delta x + \Delta \left\{ \frac{\partial H_1}{\partial v'} \right\} \delta y = 0 \quad (51)$$

where  $\Delta$  denotes the difference between the quantity in braces evaluated on each side of the corner point and  $\delta x$  and  $\delta y$  signify small variations in  $x$  and  $y$ .  $H_1$  is the integrand of the line integral portion of the functional,  $I$ .

$$H_1 = (p - p_0) \eta \eta' + C_1 G + C_2 \eta_0 (\eta \eta' - v) \quad (31)$$

At corner A, the corner point is fixed and the variables are fixed because the nozzle contour is fixed upstream of point A. Thus, all elements of the corner condition are zero and the corner condition is satisfied.

$H_1$  is not applicable at point B since  $H_1$  has values along the nozzle contour only. Therefore, the value of  $H_1$  is identically zero on both sides of corner B and the corner condition is satisfied identically.

At point C, the corner point is not fixed, so  $\delta x$  and  $\delta y$  must remain arbitrary. Therefore the coefficients of  $\delta x$  and  $\delta y$  must each be zero.

$$\Delta \left\{ H_1 - y' \frac{\partial H_1}{\partial y'} \right\} = 0 \quad (250)$$

$$\Delta \left\{ \frac{\partial H_1}{\partial y'} \right\} = 0 \quad (251)$$

Since  $H_1$  is exactly zero along the boundary BC, the quantities in braces are identically zero on that side of the corner. Therefore, the quantity in braces must also be zero at point C when evaluated along the line AC.

$$(p - p_0) \eta \eta' + C_1 G + C_2 \eta \rho (u \eta' - v) - y' \left\{ (p - p_0) \eta + C_1 G_{\eta'} + C_2 \eta \rho u \right\} = 0 \quad (252)$$

$$(p - p_0) \eta + C_1 G_{\eta'} + C_2 \eta \rho u = 0 \quad (253)$$

Equation (252) is reduced by applying equation (253) and the equation of the streamline at the nozzle contour, to obtain

$$(p - p_0) \eta \eta' + C_1 G = 0 \quad (254)$$

or, rearranging to determine the value of  $C_1$ , and using  $\eta' = v/u$ ,

$$C_1 = - \frac{(p_c - p_0) \eta_c v_c}{u_c G_c} \quad (54)$$

Substituting the value of  $C_1$  into equation (253) and rearranging to determine the value of  $C_2$  yields

$$C_{2c} = \frac{\frac{(p_c - p_0) \eta_c v_c}{u_c G_c} G_{\eta'} - (p_c - p_0) \eta_c}{\eta_c \rho_c u_c} \quad (255)$$

or

$$c_{2_c} = - \frac{(p_c - p_0) \left\{ 1 - \frac{v_c}{u_c G_c} \left( \frac{\partial G}{\partial \eta} \right)_c \right\}}{\rho_c v_c} \quad (55)$$

# APPENDIX IV THE TRANSVERSALITY CONDITION

## 1. GENERAL

For an optimum nozzle contour, the thrust must be at a maximum, and therefore cannot change with slight variations of the variables along the boundary lines. Calculus of variations expresses this condition in the transversality equation, written here for  $m$  dependent variables,

$$\xi \delta x + \eta \delta y + \sum_{k=1}^m \zeta_k \delta z_k \quad (256)$$

where  $x$  and  $y$  are the independent variables,  $z_k$  ( $k = 1 \dots, m$ ) represents the dependent variables, and

$$\begin{aligned} \xi = & \sum_{k=1}^m p_k (K_2) q_k + y' [K_2 - \sum_{k=1}^m p_k (K_2) p_k] - y' E (K_1, y) - \\ & - \sum_{k=1}^m z_k' E (K_1, z_k) \end{aligned} \quad (257)$$

$$\eta = [K_2 - \sum_{k=1}^m q_k (K_2) q_k] - y' \sum_{k=1}^m q_k (K_2) p_k + E (K_1, y) \quad (258)$$

$$\zeta_k = -(K_2)_{q_k} + y' (K_2)_{p_k} + E (K_1, z_k) \quad (k = 1, \dots, m) \quad (259)$$

$$E (K_1, y) = (K_1)_y - \frac{d}{dx} \left\{ (K_1)_{y'} \right\} \quad (260)$$

$$E (K_1, z_k) = (K_1)_{z_k} - \frac{d}{dx} \left\{ (K_1)_{z_k'} \right\} \quad (261)$$

$$y' = \frac{dy}{dx} \quad (262)$$

$$z'_k = \frac{dz_k}{dx} = p_k + y' q_k \quad (263)$$

$$p_k = \frac{\partial z_k}{\partial x} \quad (264)$$

$$q_k = \frac{\partial z_k}{\partial y} \quad (265)$$

This transversality equation is based on  $K_1$  defined as the integrand of the line integral of the functional  $I$ , with the line integral taken in the positive sense around the region ABC.  $K_2$  is the integrand of the area integral of the functional  $I$ . Therefore, in the present case

$$K_1 = - (p-p_0)nn' - C_1 G - C_2 np(un'-v) \text{ along CA} \quad (266)$$

$$K_1 = 0 \quad \text{along AB \& BC} \quad (267)$$

$$K_2 = H_2 = \sum_{i=1}^8 h_i L_i \quad (32)$$

The integrand  $K_2$  is equal to zero and  $K_1$  does not contain any partial derivatives of the dependent variables with respect to  $x$  or  $y$ .

Therefore equation (256) may be rewritten as

$$\begin{aligned} & \left\{ \sum_{k=1}^8 p_k w_k - y' E(K_1, y) - \sum_{k=1}^8 z'_k (K_1)_{z_k} \right\} \delta x + \\ & + \left\{ \sum_{k=1}^8 q_k w_k + E(K_1, y) \right\} \delta y + \\ & + \sum_{k=1}^8 \left\{ -w_k + (K_1)_{z_k} \right\} \delta z_k = 0 \end{aligned} \quad (268)$$

where

$$w_k = (K_2)_{q_k} - y' (K_2)_{p_k} \quad (269)$$

## 2. THE TRANSVERSALITY CONDITION ALONG AB

Along the boundary line AB, all dependent and independent variables are fixed since AB is a right-running characteristic from point A and the nozzle contour upstream of point A is fixed. Therefore, the variations  $\delta x$ ,  $\delta y$  and  $\delta z_k$  are all zero and the transversality condition is satisfied.

## 3. THE TRANSVERSALITY CONDITION ALONG BC

Along the boundary line BC,  $K_1$  is identically zero so equation (268) reduces to

$$\sum_{k=1}^8 p_k W_k \delta x + \sum_{k=1}^8 q_k W_k \delta y + \sum_{k=1}^8 W_k \delta z_k = 0 \quad (270)$$

The coefficients of each of the variations must equal zero if the nozzle contour is optimum since the variations are arbitrary along BC. Therefore, each of the  $W_k$  must be equal to zero to make the last term zero.

$$W_k = (K_2)_{q_k} - y'(K_2)_{p_k} = 0 \quad (k=1, \dots, 8) \quad (271)$$

Setting the coefficients of the variations of gas properties to zero results in the following equations applicable along the boundary line BC.

$$h_3 - y' h_2 + h_4 (v - y' u) = 0 \quad (56)$$

$$h_1 y (v - y' u) - h_4 a^2 (v - y' u) = 0 \quad (57)$$

$$h_2 (v - y' u) - h_1 y y' = 0 \quad (58)$$

$$h_3 (v - y' u) + h_1 y = 0 \quad (59)$$

Variations in particle properties are applicable only in the region

where particles are present. Thus, setting the coefficients of the variations of particle properties to zero results in the following equations which apply along the portion of the boundary between points B and E.

$$-h_6 \rho_p v_p + h_5 y y' \rho_p + h_6 y' \rho_p u_p = 0 \quad (272)$$

$$-h_5 y \rho_p - h_7 \rho_p v_p + h_7 y' \rho_p u_p = 0 \quad (273)$$

$$-h_5 y v_p + h_5 y y' u_p = 0 \quad (274)$$

$$-h_8 \rho_p v_p + h_8 y' \rho_p u_p = 0 \quad (275)$$

which reduce to

$$h_5 (y' u_p - v_p) = 0 \quad (60)$$

$$h_6 (y' u_p - v_p) + h_5 y y' = 0 \quad (61)$$

$$h_7 (y' u_p - v_p) - h_5 y = 0 \quad (62)$$

$$h_8 (y' u_p - v_p) = 0 \quad (63)$$

The variations of  $x$  and  $y$  do not provide any additional conditions. Both the coefficients of  $\delta x$  and  $\delta y$  go to zero when  $\dot{w}_k$  is set to zero. Thus, the entire transversality equation is satisfied along BC when equations (56) through (63) are satisfied.

#### 4. THE TRANSVERSALITY CONDITION ALONG CA

Along the nozzle contour CA, no particles are present, and thus variations of particle properties are not applicable. Using equation (268) and setting the coefficients of gas property variations equal to zero results in the following equations.

$$h_2(un'-v) + h_1\eta\eta' - C_2\eta\eta' = 0 \quad (276)$$

$$h_1\eta - h_3(un'-v) - C_2\eta = 0 \quad (277)$$

$$h_1\eta(un'-v) - h_4a^2(un'-v) + C_2\eta(un'-v) = 0 \quad (278)$$

$$h_3 - \eta'h_2 - h_4(un'-v) + \eta\eta' + C_1G_p = 0 \quad (279)$$

Along CA, the gas streamline equation  $un'-v = 0$  applies and equations (276) through (279) reduce to

$$h_1 = C_2 \quad (72)$$

$$uh_3 - vh_2 + v\eta + uC_1G_p = 0 \quad (73)$$

Setting the coefficient of the variation  $\delta x$  in equation (268) to zero yields

$$\begin{aligned} & u_x [h_2\rho v - h_1\eta\eta' - h_2\rho un'] + v_x [h_1\rho\eta + h_3\rho v - h_3\rho un'] + \\ & + p_x [h_3 - h_2\eta' + h_4v - h_4un'] + \rho_x [h_1\eta v - h_1\eta un' - \\ & - h_4a^2v + h_4a^2un'] + (p-p_0)\eta'\eta' + C_1G_\eta\eta' + C_2\rho(un'-v)\eta' - \\ & - \eta' \frac{d}{dx} [(p-p_0)\eta + C_1G_\eta + C_2\rho u] - \frac{du}{dx} [-C_2\eta\eta'] - \\ & - \frac{dv}{dx} [C_2\rho] + \frac{dp}{dx} [\eta\eta' + C_1G_p] - \frac{dp}{dx} [C_2\eta(un'-v)] = 0 \end{aligned} \quad (280)$$

Using the definition of a total derivative,

$$\frac{dF}{dx} = \frac{\partial F}{\partial x} + \eta' \frac{\partial F}{\partial \eta} \quad (281)$$

and equations (276) through (279) and the equation of a streamline,  $u\eta' - v = 0$ , equation (280) is reduced to

$$\begin{aligned} & -\eta\rho u \frac{dC_2}{dx} + C_1 G_\eta - C_1 \frac{dG_\eta}{dx} + C_1 p_\eta G_p - p_x \eta - \\ & - C_2 \left\{ \frac{d(\eta\rho u)}{dx} - \eta' \eta\rho u_\eta + \eta\rho v_\eta \right\} = 0 \end{aligned} \quad (282)$$

Using the continuity equation

$$\begin{aligned} \eta\rho v_\eta &= -\eta\rho u_x - \eta\rho p_x - \eta v_\rho_\eta - \rho v = \\ &= -\eta\rho u_x - \eta\rho p_x - \eta\eta' u\rho_\eta - \eta' u\rho \end{aligned} \quad (283)$$

and

$$\frac{d(\eta\rho u)}{dx} = \eta\rho u_x + \eta\rho p_x + \eta'\eta\rho u_\eta + \eta'\eta u\rho_\eta + \eta' \rho u \quad (284)$$

the term in the brackets  $\left\{ \right\}$  goes to zero. Further, with no particles present, the momentum equations can be written as

$$p_x = -\rho u u_x - \rho v u_\eta = -\rho u \frac{du}{dx} \quad (285)$$

$$p_\eta = -\rho u v_x - \rho v v_\eta = -\rho u \frac{dv}{dx} \quad (286)$$

which together with the relationship  $C_2 = h_1$  reduce equation (282) to

$$\frac{dh_1}{dx} = \frac{du}{dx} + \frac{C_1}{\eta\rho u} \left\{ G_\eta - \frac{d}{dx} \left( \frac{\partial G}{\partial \eta} \right) - \rho u \left( \frac{\partial G}{\partial p} \right) \frac{dv}{dx} \right\} \quad (74)$$

Setting the coefficient of the variation  $\delta y$  in equation (268) to zero yields

$$\begin{aligned}
& u_{\eta} [h_2 \rho v - h_1 \eta \rho \eta' - h_2 \rho u \eta'] + v_{\eta} [h_1 \eta \rho + h_3 \rho v - h_3 \rho u \eta'] + \\
& + p_{\eta} [h_3 - h_2 \eta' + h_4 v - h_4 u \eta'] + \rho_{\eta} [h_1 \eta v - h_1 \eta u \eta' - \\
& - h_4 a^2 v + h_4 a^2 u \eta'] - (p - p_0) \eta' - C_1 G_{\eta} - C_2 \rho (u \eta' - v) + \\
& + \frac{d}{dx} [(p - p_0) \eta + C_1 G_{\eta}' + C_2 \eta \rho u] = 0
\end{aligned} \tag{287}$$

Using the streamline equation and equations (276) through (279) reduces equation (287) to

$$\begin{aligned}
& -\eta \rho u \frac{dC_2}{dx} + C_1 G_{\eta} - C_1 \frac{dG_{\eta}}{dx} + C_1 p_{\eta} G_p - p_x \eta - \\
& - C_2 \left\{ \frac{d(\eta \rho u)}{dx} - \eta' \eta \rho u_{\eta} + \eta \rho v_{\eta} \right\} = 0
\end{aligned} \tag{282}$$

which is the same result as obtained for the variation in  $x$ . The transversality equation (74) therefore accounts for variations in both  $x$  and  $y$ .

## REFERENCES

1. Guderley, G. and Hantsch, E., "Beste Formen für Achsensymmetrische Überschallschubdüsen," *Z. Flugwiss.*, Vol. 3, 1955, pp. 305 - 313.
2. Rao, G. V. R., "Exhaust Nozzle Contour for Optimum Thrust," *Jet Propulsion*, Vol. 28, 1958, pp. 377 - 382.
3. Rao, G. V. R., "Spike Nozzle Contour for Optimum Thrust," *Ballistic Missile and Space Technology*, Vol. 2, edited by C. W. Morrow, Pergamon Press, New York, 1961, pp. 92 - 101.
4. Guderley, G., "On Rao's Method for the Computation of Exhaust Nozzles," *Z. Flugwiss.*, Vol. 7, 1959, pp. 345 - 350.
5. Guderley, K. G. and Armitage, John V., "A General Method for the Determination of Best Supersonic Rocket Nozzles," Paper presented at the Symposium on Extremal Problems in Aerodynamics, Boeing Scientific Research Laboratories, Seattle, Washington, December 3 - 4, 1962.
6. Guderley, K. G. and Armitage, J. V., "General Approach to Optimum Rocket Nozzles," Chap. 11, Theory of Optimum Aerodynamic Shapes, edited by Angelo Miele, Academic Press, New York, 1965.
7. Hoffman, J. D. and Thompson, H. D., "A General Method for Determining Optimum Thrust Nozzle Contours for Gas-Particle Flows," *AIAA Journal*, Vol. 5, No. 10, Oct. 1967, pp. 1886 - 1887.
8. Hoffman, J. D., "Optimum Thrust Nozzle Contours for Gas-Particle Flows," Report No. TM-66-2, Jet Propulsion Center, Purdue

University, March 1966.

9. Hoffman, J. D., "A General Method for Determining Optimum Thrust Nozzle Contours for Chemical Reacting Gas Flows," AIAA Journal, Vol. 5, No. 4, April 1967, pp. 670 - 676.
10. Hoffman, J. D., "Optimum Thrust Nozzle Contours for Chemical Reacting Gas Flows," Report No. TM-66-3, Jet Propulsion Center, Purdue University, April 1966.
11. Scofield, M. P. and Hoffman, J. D., "Maximum Thrust Nozzles for Rotational or Nonequilibrium Simple Dissociating Gas Flows Including Boundary Layer Effects," Report No. AFAPL-TR-69-85, Vol. 1 and 2, Air Force Aero Propulsion Laboratory, Wright-Patterson Air Force Base, Ohio, October 1969.
12. Humphreys, R. P., Thompson, H. D. and Hoffman, J. D., "Design of Maximum Thrust Plug Nozzles for Fixed Inlet Geometry," Report No. AFAPL-TR-70-47, Air Force Aero Propulsion Laboratory, Wright-Patterson Air Force Base, Ohio, June 1970.
13. Johnson, G. R., Thompson, H. D. and Hoffman, J. D., "Design of Maximum Thrust Plug Nozzles with Variable Inlet Geometry," Report No. AFAPL-TR-70-75, Vol. 1 and 2, Air Force Aero Propulsion Laboratory, Wright-Patterson Air Force Base, Ohio, October 1970.
14. Kliegel, J. R. and Nickerson, G. R., "Axisymmetric Two-Phase Perfect Gas Performance Program," Report No. 02874-6006-R000, TRW Systems, April 1967.
15. Kliegel, J. R. and Nickerson, G. R., "Flow of Gas-Particle Mixtures in Axially Symmetric Nozzles," Progress in Astronautics

- and Rocketry, Vol. 6, Detonation and Two-Phase Flow, pp. 173-194, Academic Press, New York, 1962. Also ARS preprint 1713-61, April 1961.
16. Sauerwein, H. and Fendeli, F. E., "Method of Characteristics in Two-Phase Flow," *Physics of Fluids*, Vol. 8, August 1965, pp. 1564 - 1656.
  17. Miele, Angelo, Theory of Optimum Aerodynamic Shapes, Academic Press, New York, 1965.
  18. Elsbernd, A. A. and Hoffman, J. D., "Design of Maximum Thrust Axisymmetric Nozzles with Two-Phase Flow, Vol. II, Computer Program Manual," Report No. AFAPL-TR-71-00, Air Force Aero Propulsion Laboratory, June 1971.